Proton Conductor-Supported Electrochemical Catalysts for Vehicle Emission Control

(プロトン導電体を触媒担体に使用した自動車排ガス触媒)

DONG, Xue

(董　雪)

Doctor of Engineering

Graduate School of Environmental Studies, Nagoya University

(名古屋大学大学院環境学研究科　博士(工学))

2013

ABSTRACT

With increasing vehicle population and concern over environmental issue, emission standards for hydrocarbon, carbon monoxide, and nitrogen oxides are established and tensed world widely. To meet the stringent standards, catalysts that can effectively remove pollutions from the vehicle exhausts in a relative low temperature while reducing the costs of the catalyst became a hot topic of research in recent years. In this research, using proton conductive material $Sn_{0.9}In_{0.1}P_2O_7$ as a novel support, ultra low loading $Pt/Sn_{0.9}In_{0.1}P_2O_7$ and $PtRh/Sn_{0.9}In_{0.1}P_2O_7$ electrochemical catalysts were developed and tested, and the involved an innovative mixed potential mechanism was carefully examined with other proton conductive materials.

Firstly, the two way catalysis has been investigated on the propane oxidation reaction in Chapter 2. $Sn_{0.9}In_{0.1}P_2O_7$ was used as the electrolyte in the electrochemical cell; the cell performance showed that an EMF of 332 mV and a short-circuit current of 17 $mA\,cm^{-2}$ were achieved even when the concentration of propane and O_2 concentration was at ppm levels. The electrochemical activation of oxygen also occurred under open-circuit conditions when both H_2O and O_2 were present in the reaction system, which is interpreted as a mixed potential mechanism. This phenomenon was then applied to $Pt/Sn_{0.9}In_{0.1}P_2O_7$ catalysts. Compared with the Pt/γ -Al_2O_3 catalysts, $Sn_{0.9}In_{0.1}P_2O_7$ catalysts showed higher catalytic activity at low temperatures and smaller quantities of Pt. The loading amount of Pt was significantly reduced by the impregnating Pt on the $Sn_{0.9}In_{0.1}P_2O_7$, while remaining high activity for propane. The propane conversion reached approximately 90% at 400 °C even for 0.01 wt% Pt. Meanwhile, poor activities of propane over the $MO_x/Sn_{0.9}In_{0.1}P_2O_7$ catalysts

further confirmed the electrochemical mechanism. The results shows Pt/ $Sn_{0.9}In_{0.1}P_2O_7$ could be a promising solution for the two way catalysis.

Secondly, propane oxidation and NO reduction at the proton conductor-electrocatalyst interface have been investigated using electrochemical cells and impregnated Pt/ $Sn_{0.9}In_{0.1}P_2O_7$ catalysts. In study of Chapter 3, in an electrochemical cell, propane was oxidized to CO_2 through the electrolysis of H_2O vapor at the anode. NO was reduced to N_2O through the reaction of proton with electron at the cathode. These electrochemical reactions also occurred at the same electrode in a half-cell when propane, H_2O, and NO were present in the reaction system. This phenomenon was further applicable to the Pt/$Sn_{0.9}In_{0.1}P_2O_7$ catalyst. Compared with a Pt/γ-Al_2O_3 catalyst, this catalyst showed significantly larger TOF values for Pt, thus providing higher catalytic activity for both propane and NO at low temperatures and smaller quantities of Pt. The addition of Rh to Pt further enhanced the NO reduction activity by promoting the dissociative adsorption of NO at 300 °C or higher. With such activity, the Pt-Rh/$Sn_{0.9}In_{0.1}P_2O_7$ catalyst (0.01 wt% Pt, 0.005 wt% Rh) exhibited $T_{50\%}$ of 285 and 355 °C for propane oxidation and NO reduction, respectively. Finally, the influence of the O_2 concentration in the reactant gas and its SV on the activity of Pt-Rh/$Sn_{0.9}In_{0.1}P_2O_7$ catalyst was also examined.

Finally, the relationship between the activity of the proton conductors-supported Pt-Rh catalysts for propane+NO+O_2 reaction and proton conduction in the used catalyst supports was investigated to demonstrate the reaction scheme based on the mixed potential mechanism. FNPO, SIPO, SAPO, and SMPO, which have a similar BET surface area and particle size but show different proton conductivities, were used as catalyst supports. The activity of these catalysts was significantly dependent on the

catalyst support species. $T_{50\%}$ for propane oxidation was 313, 330, 405, and 550 °C for Pt-Rh/FNPO, Pt-Rh/SIPO, Pt-Rh/SAPO, and Pt-Rh/SMPO, respectively. $T_{50\%}$ for NO reduction was 330, 386, 465, and over 600 °C for Pt-Rh/FNPO, Pt-Rh/SIPO, Pt-Rh/SAPO, and Pt-Rh/SMPO, respectively. Furthermore, Pt-Rh/FNPO and Pt-Rh/SIPO maintained high propane and NO conversions in the tested SV range, whereas Pt-Rh/SMPO showed propane and NO conversions of 10% or less at all the tested SV values. This dependence on the catalyst support species could be successfully explained by incorporating the difference in proton conduction among the catalyst supports into the mixed potential mechanism. According to this new mechanism, since protons migrate from the anodic site to the cathodic site through the proton conductor, a higher proton conductivity results in a larger short-circuit current of the local galvanic cell. In addition, since the anodic and especially cathodic potentials are determined by the rate of the proton exchange reaction between the reactant gas and the lattice oxide ion, the faster proton mobility causes the higher open-circuit voltage of the local galvanic cell. Also, we emphasize that the use, especially of FNPO, as the catalyst support could reduce significantly the Pt and Rh content while maintaining high catalytic activity.

TABLE OF CONTENTS

LIST OF FIGURES, TABLES, AND SCHEMES

Chapter I

Chapter II

Chapter III

Chapter IV

CHAPTER I
General Introduction

1.1 Environmental Issues and Vehicle Emission Control

1.1.1 The important role of vehicle emission control

At the beginning of 2013, a new term PM2.5 (particles with an aerodynamic diameter of 2.5 μm or less, also called fine particle mater) suddenly became known by many people in Japan. The particulate matter is linked with numerous health problems including asthma, bronchitis, acute and chronic respiratory symptoms, and premature deaths, according to the US environmental protection agency (EPA). Extremely high concentration of PM2.5 in China not only upsets the Chinese, but also raises health concerns among neighboring parts of Asia, especially in Japan and Korea. Many regions in Japan have reported fairly high PM2.5 levels, which are believed to be floated from mainland China. One of the main sources for the fine particulate matters, according to researchers in China, is found to be vehicle emissions, especially in the highly populated urban areas [1-3].

Assuredly, the PM2.5 is not the only air pollution problem that vehicles exhaust causes. The major exhaust pollutants from the tailpipe and their influences on people's health are as follows according to the EPA:

Hydrocarbons (HCs), resulting from partially burned fuel molecules in the engine. Hydrocarbons can react with nitrogen oxides and under the sunlight, which forms the

ground-level ozone. Ozone is a major component of chemical smog, irritating the eyes, damaging the lungs, and causing various respiratory problems. It is the most widespread and intractable urban air pollution problem. Besides, a number of exhaust hydrocarbons are also toxic by themselves.

Nitrogen oxides (NO_x), produced by the oxidation of nitrogen from air in an engine, they do harm in several aspects: (1) precursors to the formation of ozone, (2) contributor to the formation of acid rain, and (3) sources of particular matters in the form of secondary nitrates, which are caused by reaction between NO_x and ammonia or moist.

Carbon monoxide (CO), produced from incomplete combustion when carbon in the fuel is partially oxidized rather than fully oxidized to carbon dioxide (CO_2). Carbon monoxide is toxic by influencing the oxygen transfer in blood and it is particularly dangerous to persons with heart diseases.

Carbon dioxide (CO_2), not directly impairing human health, but it is a "greenhouse gas" that contributes to the tendency of global warming.

As vehicle population grows and the cities become more congested, vehicle emissions become a more and more serious problem nowadays. However, it is easy to notice that the already developed countries, even with a large vehicle numbers, are less likely suffering from pollution of those vehicle emissions, compared with those developing countries. The reason is the pollution from the vehicle emissions is provided to be controllable through the catalytic exhaust gas after-treatment, with the efforts of numerous automobile manufacturers, governments, catalyst suppliers, petroleum refiners, as well as the academic researchers. Today, exhaust catalysts are found on nearly every passenger cars, light- and medium-duty trucks, and even some heavy-duty trucks in US, Europe, Japan, and other regions, and the rapidly embraced by the India

and China.

1.1.2 History and status of vehicle emission control regulations

With the increasing concern over the environmental problems caused by the vehicle emissions, emission control standards are established in world wide. Substantial improvements have been made in for reducing the tailpipe emissions, since the original Clean Air Act passed in the US in 1970s. Meanwhile, the emission control regulations today have been much tightened. New regulations are based on the improvements of application of catalyst technologies, which also have become the drive force to motive the academic research and commercialization of vehicle catalyst technologies.

In the US, Congress passes the Clean Air Act in 1970s. The pollutants controlled are CO, VOC (volatile organic compounds), and NO_x. In the following years, the emission standards were tightening in several steps, and Federal "Tier 1" regulations and "Tier 2" standards are being started in 1994 and 2004 respectively. On the other hand, the state of California has established more stringent vehicle emissions standards specially, which were adopted as references by worldwide environmental legislation. The standard refers to LEV (Low Emission Vehicle), ULEV (Ultra LEV), SULEV (Super Ultra LEV), and ZEV (Zero Emission Vehicle). According to the US Department of Energy, from the year 1970 to 2005, the emissions of CO, NO_x and VOC had been reduced by 84%, 75% and 87% respectively.

In the European Union, Emission standards (so called "Euro standards") were first initiated in 1992, one year before the formally establish of EU. Dependent on the type of vehicles and the fuel (diesel, petrol, and gas), different standards were established and amended. The Euro standards also give limitation on the smoke. The Euro 5 and Euro 6 standards are going into effect in two years, for the cars and light duty vehicles

respectively. Besides of European Union countries, the standards of European are also widely adopted by the other countries, such as China, India and Russia, with a delay time of several years.

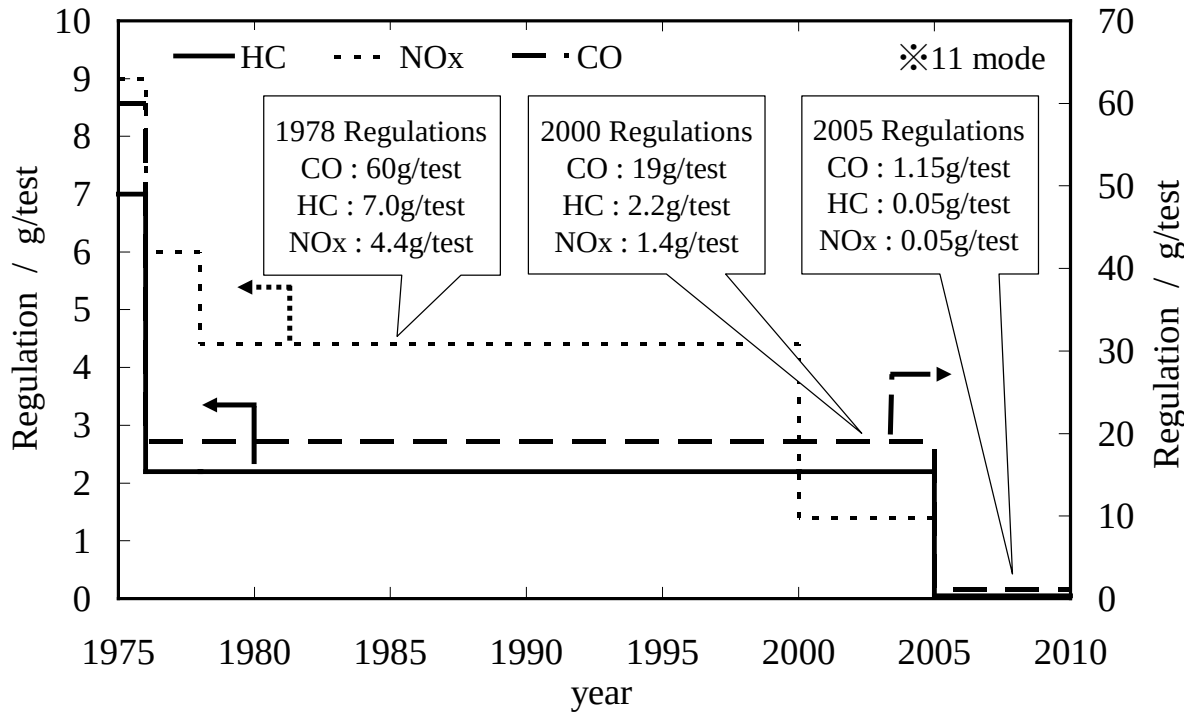

Figure 1-1 The emission control standards of gasoline automobiles in Japan.

As a leading country in the green technology of automobile, Japan also established the emission standards in 1978 (Fig.1-1), and the Motor Vehicle NO_x Law were passed in 1992 to deal with the NO_x pollution problem in urban areas, which was then amended to Automotive NO_x and PM Law in 2002. The emission standards for gasoline automobiles are also showed in the Figure 1-1.

Those worldwide established regulations impact on both the industrial and academic fields. The cost of the automobiles increased due to the complicated emission control strategies and high effective catalysts are demanded.

1.2 Introduction of Emission Control Catalysts

One of the first efforts at controlling pollution from vehicles was the positive crankcase ventilation system, which draws unburned hydrocarbons in into the engine's intake tract to burn and remove[4]. However this kind of engine technologies can hardly comply with the regulations on vehicle exhaust; thus, the catalyst converters were widely introduced on commercial automobiles in the U.S in 1975. This addition catalytic device, which works by carry a chemical reaction over catalysts in the exhaust, were once considered as an interim measures, since the unburned hydrocarbons could be removed by the improvement of engines. However, with the development of the environmental chemistry, the toxicity of NO_x and the other pollutions need to be removed from the exhaust was discovered gradually. Advanced catalysts, as the heart of an emission control system, are still continued to be used commonly in kinds of motor vehicles.

1.2.1 Two way catalysts

Oxidation catalysts (two way catalysts) are designed to oxidize unburned harmful hydrocarbons, as well as carbon monoxide into water and carbon dioxide. Restrictive regulations toward the HCs emissions have been established worldwide, which in turn calls for the development of catalysts in order to meet the regulation. Palladium and platinum catalysts supported on silica and alumina supports are used to perform the complete oxidation.

$$CO + O_2 \rightarrow CO_2$$

$$C_mH_n + (1 + n/4)O_2 \rightarrow mCO_2 + n/2H_2O$$

The catalytic converters based on this type of catalysts were once world widely used on gasoline engines until 1980s, and still can be found in some developing countries. Today, although for certain applications two way catalysts have been superseded by three way catalyst, they are still widely used not only in the diesel engines and gasoline powered industrial equipments, but also in the newly-developed LPG (Liquefied Natural Gas), CNG (Compressed Natural Gas) engines[5, 6]. However, the number of efficiency toward total hydrocarbons (THC) is normally around 80%, which can hardly meet the tensing requirements. Meanwhile, as an already highly developed industrial technology, the potential of two way catalysts based on the traditional mechanism is limited. Therefore, it is becoming necessary to develop a highly effective two way catalysts based on new mechanism.

1.2.2 Three way catalysts

Compared with the two-way catalysts, three-way catalysts (TWCs) are the most widely used solution to purify hydrocarbons, carbon oxide, and nitrogen oxides in the exhaust of gasoline engines [7-9]. In the three-way catalysts, unburned hydrocarbons and carbon monoxide are oxidized, and meanwhile produced nitrogen oxides are reduced. The TWCs promote the following reactions for CO, HC, and NO_x in the exhaust [10]:

$$CO + 1/2O_2 \rightarrow CO_2$$

$$CO + H_2O \rightarrow CO_2 + H_2$$

$$C_mH_n + (1 + n/4)O_2 \rightarrow mCO_2 + n/2H_2O$$

$$NO(\text{or } NO_2) + H_2 \rightarrow 1/2N_2 + H_2O$$

$$(2 + n/2)NO(\text{or } NO_2) + C_nH_m \rightarrow (1 + n/4)N_2 + mCO_2 + n/2H_2O$$

Typically, the CO reaction first begins, followed by the HC and NO_x reaction.

Therefore, the ability of TWCs is determined by the catalytic activity for the HCs and NO_x reaction. For the oxidation of HCs, the activation of C-H bonds step is believed to be the key step since a considerable high Activation Energy is required. The active oxygen species (refer to the absorbed or lattice reactive oxygen atom or ions) are found to have the ability of breaking the C–H bond in hydrocarbons by most researchers [11, 12]. For the reduction of NOx, the air/fuel ratio of the exhaust should be controlled close to a stoichiometric value, which is 14.6 for a gasoline engine (Fig. 1-2) and slightly different for the engines burning other fuels. If the ratio is larger, the so called lean condition, the oxidation of the CO and hydrocarbons are favored but the conversion of NO will reduced sharply given the oxidizing conditions. When the ratio is smaller and there is less oxygen than required, so called rich conditions, the reduction of NO_x is favored at the expense of the CO and HC oxidation. Therefore, in the engines to date, the three way catalytic converters are generally combined with a computerized closed-loop feedback fuel injection system, which control the air/fuel ratio in the narrow window using the signals from the oxygen sensors.

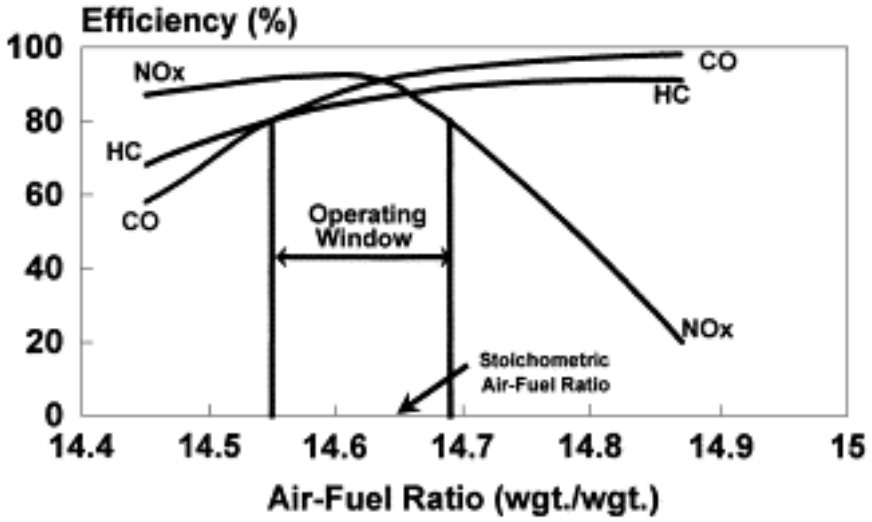

Figure 1-2 Three way catalyst: simultaneous conversion of CO, HC and NO_x.[13]

After thirty years' development, the widespread used three way catalysts in the automobile are usually composed with a ceramic or metallic monolithic substrate (honeycomb substrate) and the carried catalytic washcoat, Scheme 1-1 [14, 15]. This honeycomb structure allows a large surface area to increase the conversion efficiency, and make the exhaust can go through easily with less pressure loss. The rust structure is easily to be produced and fitted in the vehicles, and also provides high resistance to the high temperature and physical vibration. For the washcoat, it is usually composed by a supported catalytically active precious metal components (usually is the platinum group metals, abbreviated as PGMs), along with the additional oxides. The γ-Al_2O_3, modified by the oxide stabilizers, is one of the most wildly used supported materials for its large surface areas and the resistance to the high temperature and high water vapor contents in the exhaust. The PGMs (Pt, Rh, and Pd) are the active components in the catalyst to performance the oxidation and reduction. The addition of rare earth metals oxides (CeO_2 and ZrO_2), enhances the dispersion of the precious metals and plays an important role by providing oxygen storage which to some extent broadens the narrow window of air/fuel ratio for the three catalysts. The complex structure and composition of the three way catalysts make the researches in this area harder than even, since a large amount of factors should be considered in the preparation and application. The interactions can occur among the precious metals, the rare earth metals oxides, and the carrier material, or even occur between two kinds of precious metals. The mechanism involves the physical and the chemical properties of both surface and bulk of the catalysts. Those research developments will be further explained in the next sections.

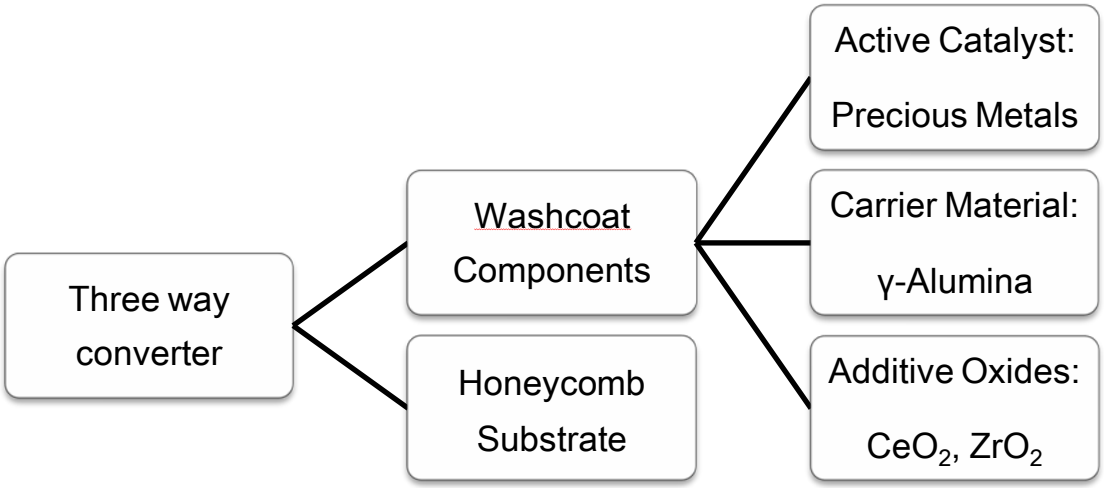

Scheme 1-1 A composition of three way converter.

1.3 Development of Vehicle Catalysts

1.3.1 Advances on precious metals

Today most catalysts used in the vehicles are the supported precious metal catalysts. At the beginning of technologies on vehicle emission control, due to the high cost of the precious metals, early researchers had screened base metal oxide catalysts carefully, especially the transition metal oxides for their activity on the combustion of hydrocarbon [16, 17]. However, all the attempts were found to be useless, since the base metals are lack of the reactivity and durability, and most importantly, the poison resistances against sulfur or lead in the exhaust. Therefore, most of the researches are devoted to the platinum group metals and great advances have been achieved.

Of the candidate platinum group metals, Ru, Ir, and Os are all tend to form oxides that easily to violate at high temperature and thus not suitable for the vehicle catalysts . For example, due to its selectivity for the NO_x, Ru was investigated thoroughly as a potential catalyst in mid-1970s. The metal was stabilized by preparation of various pure or substituted ruthenates to stop the violating [ ]. Among those attempts, impressive improvement of stability was realized, but the activity of NO reduction was weakened and more importantly the selectivity lost: large amout of NH_3 was produced. Thus, Pt and Pd are chose as the oxidation catalysts in catalytic emission controls, and Rh is chose as the reduction catalysts for NO_x.

Pt is the most widely used catalyst since the very beginning for its great stability against high temperature and activity toward hydrocarbons including olefins. Compared with Pd, Pt is less tend to react with lead and has a high resistance toward the poisoning of sulfur oxides [21]. Therefore, the Pt catalysts have been widely used in the automobile emission control system with less limitation for petroleum technologies and the other pretreatments.

On the other hand, Rh is the clear choice for NO_x control. The reason could be explained by a research carried by Taylor and Schlatter in the year 1980 [ ]. In this research, the conversions of NO, CO, and O_2 were compared among Ir, Rh, Pt, and Pd catalysts. Rh did not only achieve high NO_x conversion near stoichiometric air/fuel ratio but also retained NO_x conversion under the slight lean conditions. Furthermore, compared with other metals, Rh produced less NH_3 under the strongly reduction favored conditions. However, under a temperature equal or high than the 600 ^oC, Rh tends to react with alumina and lost its activity. The solution to inhibit this interaction was to support the Ph on the alternative supports other than the commonly used γ-Al_2O_3,

and rare earth mixed oxides of CeO_2 and ZrO_2 were believed to be a suitable choice [23, 24].

The Pt/Rh supported catalysts are the most widely used catalysts to deal with the vehicle emission, but the cost of the two components is high and the storage is limited. The less expensive Pd is also active for the oxidation of hydrocarbons and reduction of nitrogen oxides and becomes an alternative solution. However, due to its weak resistance toward the lead and sulfur, it did not apply with the TWCs in the whole decade of the 1980s, when the technology on refine of the oil was still under development. Also, in a normal Pd/Rh catalyst formulation, the surface of the Rh will be covered by the surface segregation of Pd at high temperature, which leads to the suppression of the reduction of the NO_x. Again the solution would be segregating the two metals on different support, but the complexity in the preparation was increased significantly.

Recently, considerable researches were carried to discuss the possibility of using Pd as the only formulation of the three way catalysts, since it is active for the NO_x and less expensive. Pd with WO_3 and Al_2O_3 catalyst formulations were found to have excellent N_2 selectivity [25]. The catalyst using Pd with MoO_3 and La also showed the high activity as a NO_x reduction catalyst, but the neither of them can be commercialization due to the high-temperature volatilization of MoO_3 or the narrowness of the NO_x window [26-28]. Thus, the researches indicated that Pd formulation is a promising solution for the TWCs, but additional developments are required before using it in the automobile industry.

1.3.2 Advances on additive oxides

The rare earth metal oxides are multiple functioned in the three way catalysts. The Ceria compounds can regulate properties of oxygen storage and release in the reaction, which is regarded as one of the most remarkable advances of the three-way catalyst. As we stated, for the perform the oxidation and reduction effectively, a three-way catalyst must work under atmospheres with stoichiometric air to fuel ratios (A/F), which is fluctuating since it is maintained by computer adjusted injection system. The oxygen storage materials are able to widen the A/F window by storing extra oxygen in the oxidative atmosphere and release when the oxygen is deficient, by which the conversions of NO_x, CO and HC are efficiently improved [29]. The oxygen storage capacity (OSC) of CeO_2 could be further improved by addition of lanthanum or zirconium ions into CeO_2, for more oxygen defects are introduced into the bulk. Particularly, for the ZrO_2, the zirconium ions have a smaller diameter compared with the cerium ions, and the space for the oxygen ions is further increased in the lattice cell. Therefore, the CeO_2 and ZrO_2 are added to most of the three way converters [30, 31].

According to the research, the addition of those oxides also works to promote precious metal dispersion, increase thermal stability of the alumina support, promote the water gas shift and the steam reforming reactions, and enhance catalytic activity at the interfacial reactive sites[8, 32-35].

1.3.3 Challenges in the vehicle catalysts

Although great advancements have been achieved in the past forty years, challenges are still lie ahead. With increasing vehicle population and concern over the air quality, stringent regulations are to be arranged world widely and new catalysts are required.

One of the challenges is cost control of the automobile catalyst. The activation of

propane is generally catalyzed on the Pt catalysts, and Rh is used to improve the conversion of NO. However, just as the term precious metals suggested, the Pt and Rh are very expensive for their unevenly distribution and small amount of storage around the world, which raise the cost of automotive converters productio and catalyst coating technology leverages up to 90% of total catalytic converter costs. In order to solve this problem, one approach is to use Pd as the only active metal in TWCs, which has been aggressively pursued over the past decade [36-38], but the commercialization of this system has not yet been realized. An alternative approach is to reduce the loading amount of Pt and Rh contents while maintaining high catalytic activity. Papavasiliou et al. decreased the Pt content to 0.5 wt% over γ-Al_2O_3 by using $Ce_{0.4}Zr_{0.5}La_{0.1}O_{1.9}$ as a promoter [39]. It is believed that a further reduction in these precious metals would enhance the position of TWCs as preferred emission control technologies.

Another key problem is the cold start strategy. In the first 2 minutes of a drive cycle, the catalyst cannot reach its HC light-off temperatures (about 300 ^{o}C). Consequently, nearly 50-80% of the total unburned hydrocarbons will be emitted during this period (Society of Automotive Engineer, SAE. 961954), resulting in a failure to meet future regulations. The close coupled catalyst appears to a promising cold start strategy, which is catalysts mounted close to the manifold of engines, and then it can benefit from the hot of the exhaust and thus reach light-off temperatures of hydrocarbon in a very short time. Disadvantage of the close couple is the sintering leading by a higher temperature of the exhaust and thermal durability is required [13]. The other solutions includes the electrically heated catalyst(heating a small parts of catalysts electrically by a metal substrate and shorting the light-off time [40, 41]), hydrocarbon trap (storing the unburned hydrocarbons emitting in the cold start possess and burn them after the

light-off temperature is reached [42, 43]). However, all those solutions add the complexity to the catalysts system. Therefore, a low light-off catalyst would be a promising solution.

1.4 Aim of the Thesis

1.4.1 Background of $Sn_{0.9}In_{0.1}P_2O_7$

Recently, Hibino et al. found that an anhydrous proton conductor, In^{3+}-doped SnP_2O_7 ($Sn_{0.9}In_{0.1}P_2O_7$), shows high proton conductivities between 150 and 300°C under unhumidified conditions [44]. $Sn_{0.9}In_{0.1}P_2O_7$ shows a cubic structure with SnO6 octahedral and P_2O_7 units at the corners and the edges, respectively (Fig. 1-7). Such closely packed P_2O_7 units could provide many proton bonding sites and associated transport pathways in the bulk, resulting in high proton conductivities above 0.1 S cm^{-1} between 150 and 350°C under unhumidified conditions. This material has a cubic or pseudo-cubic structure over a wide temperature range, which is characterized by SnO_6 octahedral at the corners and P_2O_7 units at the edges [45]. There are nominally no structural protons in SnP_2O_7, suggesting that protons dissolve as defects in the presence of hydrogen-containing gases. A similar proton incorporation mechanism has been proposed for Ca^{2+}- or Sr^{2+}-doped $LaPO_4$ in phosphate-based proton conductors [46, 47]. However, the proton conductivities of the $LaPO_4$-based proton conductors were much lower than those of SnP_2O_7 in the temperature range from 150 to 300°C, probably due to the difference in their constituent oxyanions ($P_2O_7^{4+}$ and PO_4^{3+}). Indeed, the previous study showed that the conductivity of $SnHPO_4$ was about three orders of magnitude

lower than that of SnP_2O_7.

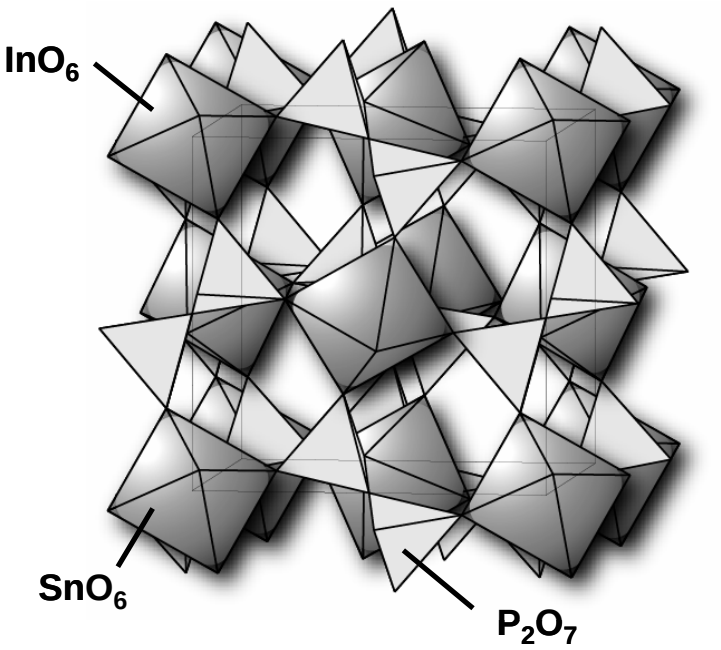

Figure 1-3 Structure of SnP_2O_7

As the electrolyte, the proton-conducting SIPO has been used as electrolyte in a direct hydrocarbon fuel cell in the previous study, and in the anode the hydrocarbons even some light hydrocarbons could be oxidized in a relatively low temperature range [48]. Furthermore, this reaction occurred accomplished with a high faradic current, at the Pt/C anode:

$$C_nH_{2n+2} + 2nH_2O \rightarrow nCO_2 + (6n+2)H^+ + (6n+2)e^-$$

It is also found that during anodic polarization of H_2O, the active oxygen specie HO· is formed from the dissociation of the water, which breaks the C-H bond by extraction of hydrogen [49, 50]. In the cathode, the oxygen is reduced on the surface of Pt/C electrode.

$$(1.5n + 0.5)O_2 + (6n+2)H+ (6n+2)e^- \rightarrow (3n + 1)H_2O$$

Consequently, high power densities were found in those fuel cells and the stability and the durability toward temperature of the fuel cell were also found appreciable. We also

recently reported that NO reacted with protons and electrons to form N_2 and H_2O at a Pt/C cathode in the similar electrochemical cell as described above [51, 52].

$$NO + 2H^+ + 2e^- \rightarrow 1/2N_2 + H_2O$$

Those research results indicated a possibility to develop an electrochemical reactor basing on those reactions, which could be used to remove the hydrocarbons and NO_x in vehicle exhaust.

1.4.2 Research Purpose

Based on these observations, it is expected that an electrochemical reactor for the HC and O_2 reaction can be developed through the oxidation and reduction reactions by short-circuiting reactor. Due to the high efficiency of the electrochemical reactor, high conversions of propane could be achieved. Furthermore, if this reactor is designed by using NO_x as the reactive gas in the cathode instead of O_2, then the three way catalysis reaction could occur. Based on this design, nano-scale electrochemical reactors can be produced by impregnating $Sn_{0.9}In_{0.1}P_2O_7$ with Pt and Rh, and then the reaction area for the HC and NO_x reaction can be drastically increased and the loading amount of Pt and Rh could be reduced. Furthermore, considering the reaction temperature of the hydrocarbon direct fuel cell, it is important for our catalysts to maintain the catalysts activity in a relatively low range while decrease the loading contents of precious metals.

The goals of the present work are to: (1) design a high efficiency electrochemical reactor based on the oxidation of HC and reduction Oxygen (NO_x) reaction, using the SIPO as the electrolyte (2) demonstrate the advantage of nanoscale electrochemical reactors formed in the surface of SIPO supported Pt (Pt/Rh) catalyst, for the HC oxidation and NO_x reduction; (3) reduce Pt and Rh loadings amounts; and (4) further

discuss the mechanism by using the other proton conductors as catalyst support.

1.4.3 Scope of Thesis

In Chapter 2, the two way catalysis has been investigated using electrochemical by using propane as the test hydrocarbon. $Sn_{0.9}In_{0.1}P_2O_7$ and Pt was used as the proton conductor and electrocatalyst, respectively. The loading amount of Pt was reduced to 0.01%. In Chapter 3, propane oxidation and NO reduction at the proton conductor-electrocatalyst interface have been investigated using electrochemical cells and impregnated catalysts. Ultra low loading amount Rh was introduced to improve the conversion of NO reduction. In Chapter 4, Propane+NO+oxygen reaction over PtRh was investigated using SnP_2O_7-based proton conductors of $Sn_{0.9}In_{0.1}P_2O_7$ (SIPO), $Sn_{0.95}Al_{0.05}P_2O_7$ (SAPO), $Sn_{0.9}Mg_{0.1}P_2O_7$ (SMPO) and $Fe_{0.5}Nb_{0.5}P_2O_7$ (FNPO) as catalyst supports, and the catalytic activity for the propane and NO reaction is related to proton conduction in the catalyst supports.

1.5 References

[1] Y. Song, Y.H. Zhang, S.D. Xie, L.M. Zeng, M. Zheng, L.G. Salmon, M. Shao, and S. Slanina, Source apportionment of PM2.5 in Beijing by positive matrix factorization, *Atmos Environ*. **40**(8), 1526-1537 (2006).

[2] Q. Wang, M. Shao, Y. Zhang, Y. Wei, M. Hu, and S. Guo, Source apportionment of fine organic aerosols in Beijing, *Atmos Chem Phys*. **9**(21), 8573-8585 (2009).

[3] B. Han, S.F. Kong, Z.P. Bai, G. Du, T. Bi, X. Li, G.L. Shi, and Y. Hu, Characterization of Elemental Species in PM2.5 Samples Collected in Four Cities of Northeast China, *Water Air Soil Poll*. **209**(1-4), 15-28 (2010).

[4] C.B. Tracy and W.W. Frank, Fuels Lubricants and Positive Crankcase Ventilation Systems, *Sae Prog Technol*. **12** 451-& (1967).

[5] J.P.A. Neeft, M. Makkee, and J.A. Moulijn, Diesel particulate emission control, *Fuel*

Process Technol. **47**(1), 1-69 (1996).

[6] P. Gelin and M. Primet, Complete oxidation of methane at low temperature over noble metal based catalysts: a review, *Appl Catal B-Environ*. **39**(1), 1-37 (2002).

[7] H.S. Gandhi, G.W. Graham, and R.W. McCabe, Automotive exhaust catalysis, *J Catal*. **216**(1-2), 433-442 (2003).

[8] M.V. Twigg, Roles of catalytic oxidation in control of vehicle exhaust emissions, *Catal Today*. **117**(4), 407-418 (2006).

[9] S.I. Matsumoto, Recent advances in automobile exhaust catalysts, *Catal Today*. **90**(3-4), 183-190 (2004).

[10] R. Moller, C.H. Onder, L. Guzzella, M. Votsmeier, and J. Gieshoff, Analysis of a kinetic model describing the dynamic operation of a three-way catalyst, *Appl Catal B-Environ*. **70**(1-4), 269-275 (2007).

[11] Y. Yazawa, H. Yoshida, N. Takagi, S. Komai, A. Satsuma, and T. Hattori, Acid strength of support materials as a factor controlling oxidation state of palladium catalyst for propane combustion, *J Catal*. **187**(1), 15-23 (1999).

[12] B. Grbic, N. Radic, B. Markovic, P. Stefanov, D. Stoychev, and T. Marinova, Influence of manganese oxide on the activity of Pt/Al2O3 catalyst for CO and n-hexane oxidation, *Appl Catal B-Environ*. **64**(1-2), 51-56 (2006).

[13] R.J. Farrauto and R.M. Heck, Catalytic converters: state of the art and perspectives, *Catal Today*. **51**(3-4), 351-360 (1999).

[14] C.J. Pereira and K.W. Plumlee, Grace Camet(R) Metal Monolith Catalytic Emission Control Technologies, *Catal Today*. **13**(1), 23-32 (1992).

[15] S.R. Gundlapally and V. Balakotaiah, Analysis of the effect of substrate material on the steady-state and transient performance of monolith reactors, *Chem Eng Sci*. **92** 198-210 (2013).

[16] J.T. Kummer, Catalysts for Automobile Emission Control, *Prog Energ Combust*. **6**(2), 177-199 (1980).

[17] J.T. Kummer, Use of Noble-Metals in Automobile Exhaust Catalysts, *J Phys Chem-Us*. **90**(20), 4747-4752 (1986).

[18] Voorhoev.Rj, J.P. Remeika, and L.E. Trimble, Perovskites Containing Ruthenium as Catalysts for Nitric-Oxide Reduction, *Mater Res Bull*. **9**(10), 1393-1404 (1974).

[19] H.S. Gandhi, H.K. Stepien, and M. Shelef, Optimization of Ruthenium-Containing, Stabilized, Nitric-Oxide Reduction Catalysts, *Mater Res Bull*. **10**(8), 837-845 (1975).

[20] G.L. Bauerle, Pinkerto.Jd, and K. Nobe, Mixed-Oxide Catalysts for Pollution-Control, *Atmos Environ*. **8**(3), 217-219 (1974).

[21] H.S. Gandhi and M. Shelef, Effects of Sulfur on Noble-Metal Automotive Catalysts, *Appl Catal*. **77**(2), 175-186 (1991).

[22] K.C. Taylor and J.C. Schlatter, Selective Reduction of Nitric-Oxide over Noble-Metals, *J Catal*. **63**(1), 53-71 (1980).

[23] H.C. Yao, H.K. Stepien, and H.S. Gandhi, Metal-Support Interaction in Automotive Exhaust Catalysts - Rh-Washcoat Interaction, *J Catal*. **61**(2), 547-550 (1980).

[24] R. Polvinen, M. Vippola, M. Valden, T. Lepisto, A. Suopanki, and M. Harkonen, The effect of Pt-Rh synergism on the thermal stability of rhodium oxide on pure alumina and Ce-ZrO_2-modified alumina-supported catalysts, *J Catal*. **226**(2), 372-381 (2004).

[25] K.M. Adams and H.S. Gandhi, Palladium Tungsten Catalysts for Automotive Exhaust Treatment, *Ind Eng Chem Prod Rd*. **22**(2), 207-212 (1983).

[26] H. Muraki, H. Shinjoh, H. Sobukawa, K. Yokota, and Y. Fujitani, Palladium Lanthanum Catalysts for Automotive Emission Control, *Ind Eng Chem Prod Rd*. **25**(2), 202-208 (1986).

[27] H. Muraki, K. Yokota, and Y. Fujitani, Nitric-Oxide Reduction Performance of Automotive Palladium Catalysts, *Appl Catal*. **48**(1), 93-105 (1989).

[28] H. Muraki, H. Shinjoh, and Y. Fujitani, Effect of Lanthanum on the No Reduction over Palladium Catalysts, *Appl Catal*. **22**(2), 325-335 (1986).

[29] H. Shinjoh, Rare earth metals for automotive exhaust catalysts, *J Alloy Compd*. **408** 1061-1064 (2006).

[30] M. Ozawa, M. Kimura, and A. Isogai, The Application of Ce-Zr Oxide Solid-Solution to Oxygen Storage Promoters in Automotive Catalysts, *J Alloy Compd*. **193**(1-2), 73-75 (1993).

[31] Y. Nagai, T. Yamamoto, T. Tanaka, S. Yoshida, T. Nonaka, T. Okamoto, A. Suda, and M. Sugiura, X-ray absorption fine structure analysis of local structure of CeO2-ZrO2 mixed oxides with the same composition ratio (Ce/Zr=1), *Catal Today*. **74**(3-4), 225-234 (2002).

[32] M. Ozawa, M. Kimura, and A. Isogai, Thermal-Stability and Characterization of Gamma-Al2o3 Modified with Rare-Earths, *J Less-Common Met.* **162**(2), 297-308 (1990).

[33] Z.R. Ismagilov, R.A. Shkrabina, N.A. Koryabkina, D.A. Arendarskii, and N.V. Shikina, Preparation and study of thermally stable washcoat aluminas for automotive catalysts., *Catalysis and Automotive Pollution Control Iv*. **116** 507-511 (1998).

[34] P. Bera, K.R. Priolkar, A. Gayen, P.R. Sarode, M.S. Hegde, S. Emura, R.

Kumashiro, V. Jayaram, and G.N. Subbanna, Ionic dispersion of Pt over CeO_2 by the combustion method: Structural investigation by XRD, TEM, XPS, and EXAFS, *Chem Mater*. **15**(10), 2049-2060 (2003).

[35] D.J. Pettigrew, D.L. Trimm, and N.W. Cant, The Effects of Rare-Earth-Oxides on the Reverse Water-Gas Shift Reaction on Palladium Alumina, *Catal Lett*. **28**(2-4), 313-319 (1994).

[36] Z. Hu, C.Z. Wan, Y.K. Lui, J. Dettling, and J.J. Steger, Design of a novel Pd three-way catalyst: Integration of catalytic functions in three dimensions, *Catal Today*. **30**(1-3), 83-89 (1996).

[37] A. Martinez-Arias, M. Fernandez-Garcia, A.B. Hungria, A. Iglesias-Juez, K. Duncan, R. Smith, J.A. Anderson, J.C. Conesa, and J. Soria, Effect of thermal sintering on light-off performance of $Pd/(Ce,Zr)_{O-x/}Al_2O_3$ three-way catalysts: Model gas and engine tests, *J Catal*. **204**(1), 238-248 (2001).

[38] G.F. Li, Q.Y. Wang, B. Zhao, and R.X. Zhou, The promotional effect of transition metals on the catalytic behavior of model $Pd/Ce_{(0.67)}Zr_{(0.33)}O_{(2)}$ three-way catalyst, *Catal Today*. **158**(3-4), 385-392 (2010).

[39] A. Papavasiliou, A. Tsetsekou, V. Matsouka, M. Konsolakis, and I.V. Yentekakis, An investigation of the role of Zr and La dopants into $Ce_{1-x-y}Zr_xLa_yO$ delta enriched gamma-Al_2O_3 TWC washcoats, *Appl Catal a-Gen*. **382**(1), 73-84 (2010).

[40] M.J. Heimrich, S. Albu, and M. Ahuja, Electrically Heated Catalysts for Cold-Start Emission Control on Gasoline-Fueled and Methanol-Fueled Vehicles, *J Eng Gas Turb Power*. **114**(3), 496-501 (1992).

[41] K. Ramanathan, S.H. Oh, and E.J. Bissett, Electrically Heated Catalysts for Hybrid Applications: Mathematical Modeling and Analysis, *Ind Eng Chem Res*. **50**(14), 8444-8467 (2011).

[42] Z.M. Gao, M.Y. Kim, J.S. Choi, C.S. Daw, J.E. Parks, and D.E. Smith, Cold-start emissions control in hybrid vehicles equipped with a passive adsorber for hydrocarbons and nitrogen oxides, *P I Mech Eng D-J Aut*. **226**(D10), 1396-1407 (2012).

[43] B.L. Yang and H.H. Kung, Reactor Trap to Remove Hydrocarbons from Engine Exhaust during Cold Start, *Environ Sci Technol*. **28**(8), 1561-1564 (1994).

[44] M. Nagao, A. Takeuchi, P. Heo, T. Hibino, M. Sano, and A. Tomitab, A proton-conducting In3+-doped SnP2O7 electrolyte for intermediate-temperature fuel cells, *Electrochem Solid St*. **9**(3), A105-A109 (2006).

[45] R.K.B. Gover, N.D. Withers, S. Allen, R.L. Withers, and J.S.O. Evans, Structure and phase transitions of SnP2O7, *J Solid State Chem*. **166**(1), 42-48 (2002).

[46] S. Gallini, M. Hansel, T. Norby, M.T. Colomer, and J.R. Jurado, Impedance spectroscopy and proton transport number measurements on Sr-substituted LaPO4 prepared by combustion synthesis, *Solid State Ionics*. **162** 167-173 (2003).

[47] K. Amezawa, Y. Tomii, and N. Yamamoto, High temperature protonic conduction in Ca-doped YPO4, *Solid State Ionics*. **162** 175-180 (2003).

[48] P. Heo, K. Ito, A. Tomita, and T. Hibino, A proton-conducting fuel cell operating with hydrocarbon fuels, *Angew Chem Int Edit*. **47**(41), 7841-7844 (2008).

[49] N.M. Markovic and P.N. Ross, Surface science studies of model fuel cell electrocatalysts, *Surf Sci Rep*. **45**(4-6), 121-229 (2002).

[50] W.S. Li, D.S. Lu, J.L. Luo, and K.T. Chuang, Chemicals and energy co-generation from direct hydrocarbons/oxygen proton exchange membrane fuel cell, *J Power Sources*. **145**(2), 376-382 (2005).

[51] M. Nagao, T. Yoshii, T. Hibino, M. Sano, and A. Tomita, Electrochemical reduction of NOx at intermediate temperatures using a proton-conducting In^{3+}-doped SnP_2O_7 electrolyte, *Electrochem Solid St.* **9**(2), J1-J4 (2006).

[52] A. Tomita, T. Yoshii, S. Teranishi, M. Nagao, and T. Hibino, Selective catalytic reduction of NOx by H-2 using proton conductors as catalyst supports, *J Catal*. **247**(2), 137-144 (2007).

CHAPTER II

Two Way Catalysis over $Sn_{0.9}In_{0.1}P_2O_7$ Catalysts

2.1 Introduction

As a major contributor to the photo-chemical smog and ozone pollution, the unburned hydrocarbons (HCs) are one of main pollutions from the internal combustion engine. To address this problem, oxidation catalysts (two way catalysts) are designed to oxidize unburned harmful hydrocarbons, as well as carbon monoxide into water and carbon dioxide. Meanwhile, stringent regulations toward the HCs emissions have been established worldwide, which in turn calls for the development of catalysts in order to comply with the regulation. Today, although for certain applications two way catalysts have been superseded by three way catalysts, they are still widely used not only in the diesel engines and gasoline powered industrial equipments, but also in some newly-developed LPG (Liquefied Natural Gas), CNG (Compressed Natural Gas) engines [1, 2]. However, the catalysts are requiring an ignition temperature 300 ^{o}C or even higher to achieve good conversions of the pollutions, especially for those light saturated hydrocarbons. Meanwhile, the temperatures of exhaust from the commercial engines are lower than 200 ^{o}C during cold-start transients, and the unburned hydrocarbons cannot be removed by the converter and therefore released directly into the atmosphere [3]. This temperature gap makes it hard to use the current catalysts to solve this problem and thus new cold start strategy is in necessary. However, as a highly

matured industrial technology, the potential of two way catalysts based on the traditional mechanism is facing its own upper limit. Thus, recently it is believed that developing of a novel hydrocarbon oxidation catalyst which can work at lower temperature is a potential solution to control emission from vehicles [4, 5].

Based on the mechanism studies on hydrocarbons oxidation, the activation of C-H bonds step is believed to be the initial and key step since a considerable high Activation Energy is required in this step [6-8]. Catalyzed by the catalysts, where in the case of vehicles emission control usually precious metals (Pt, Rh, and Pd) are adopted, the generated active oxygen species (or reactive oxygen species, refer to the absorbed or lattice reactive oxygen atom or ions) are regarded with breakage of the C-H bond in hydrocarbons by most researchers [9, 10]. Interestingly, the active oxygen species also form in some electrochemical processes. During the research of low temperature fuel cell, our lab has found a proton conductive material $Sn_{0.9}In_{0.1}P_2O_7$ (SIPO) [11]. As a pure proton conductor, this material has high proton conductivity in the temperature around 200 ^oC, and the proton conductivity could be maintained even at a temperature higher than 200 ^oC as an oxides. This proton conductive material was used as electrolyte in a proton exchange membrane fuel cell in the previous study, and in the anode the hydrocarbons even some light hydrocarbons could be completely oxidized in a relatively low temperature range [12]. At a Pt/C anode, this reaction occurred and a high faradic current was generated:

$$C_nH_{2n+2} + 2nH_2O \rightarrow nCO_2 + (6n+2)H^+ + (6n+2)e^- \qquad (1)$$

It is also found that during anodic polarization of H_2O, the active oxygen specie $HO\cdot$ is formed from the electrochemical dissociation of water, which was regarded to the breakage of C-H bond [13, 14]. In the cathode, the oxygen is reduced on the surface of

Pt/C electrode:

$$(1.5n + 0.5)O_2 + (6n+2)H+ (6n+2)e^- \rightarrow (3n + 1)H_2O \qquad (2)$$

Consequently, high power densities were generated in the whole fuel cell test, and the stability and the durability toward temperature of the fuel cell were also found appreciable. The research results indicated a possibility to develop an electrochemical reactor basing on those reactions, which could be used to remove the hydrocarbon in the vehicle exhaust.

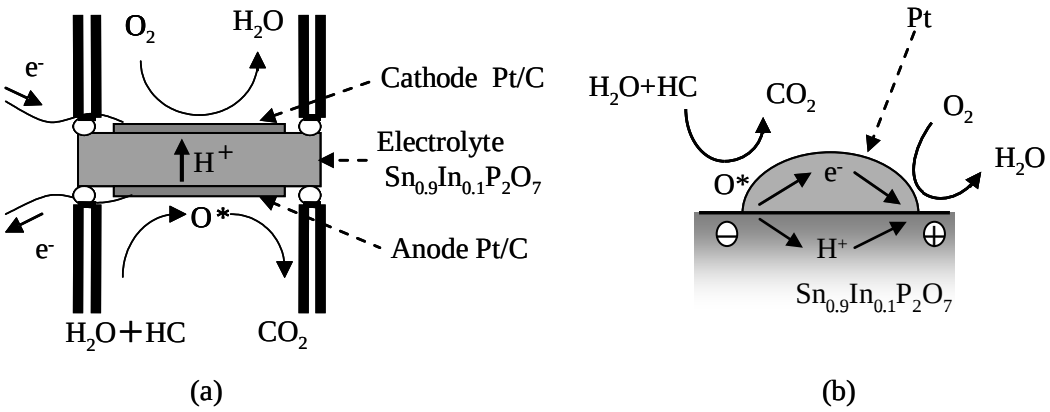

Scheme 2-1. Schematic illustrations of (a) fuel cell and (b) local electrochemical cell.

A fuel cell using $Sn_{0.9}In_{0.1}P_2O_7$ as the electrolyte (Scheme 2-1, a) was designed to testify the possibility of the electrochemical reaction, and the cell performance using various concentrations of propane and O_2 was obtained [15]. The electrochemical cell performance was tested separately at 300 ^oC using propane and O_2 with different concentration. An EMF of 332 mV and a short-circuit current of 17 mA cm^{-2} were observed under the 1000 ppm concentration of propane and 5000 ppm of O_2. Those results suggested a high theoretic possibility of a fuel-cell type reactor working with low concentration of exhaust.

Also, if the reaction followed this electrochemical scheme, in a fuel cell using $Sn_{0.9}In_{0.1}P_2O_7$ electrolyte, the propane will be oxidized to CO_2 at anodic sites (Reaction

(1)) on the Pt/C electrode, and on the same electrode the reduction of oxygen also occur at cathodic sites through Reaction (2). As a result, a local galvanic cell is formed at one Pt particle (Scheme 2-1, b). The kind of cell is short-circuited due to the conductivity of the Pt, and therefore the reaction rate on the two electrodes should be the same- a mixed potential is produced. The similar phenomena have been reported on the gas senor working in the mixtures of various gases [16, 17]. To testify the assumption, the polarization curves of the propane oxidation and oxygen reduction were measured separately on a Pt/C electrode at different temperature, and the mixed potentials were estimated from the intersection points of the anodic and cathodic polarization curves. The results were ploted in Figure 2-1. Meanwhile, the practical open-circuit potentials of the electrochemical reaction for the Pt/C electrode were measured in a mixture gas of 1000 ppm propane, 5000 ppm oxygen and 3% H_2O diluted with Ar at the same temperature. The results were also plotted in the Fig.2-1. We could find that the two series of data points were in accordance with each other. That is to say, at each temperature, the mixed potential from the propane oxidation oxygen reduction reaction on the anodic electrode and on the cathodic electrode is almost equal to the real open circuit potential on anodic and cathodic sites of the electrode. The results demonstrate the reactions occur in the electrochemical route we assumed in the scheme 2-1.

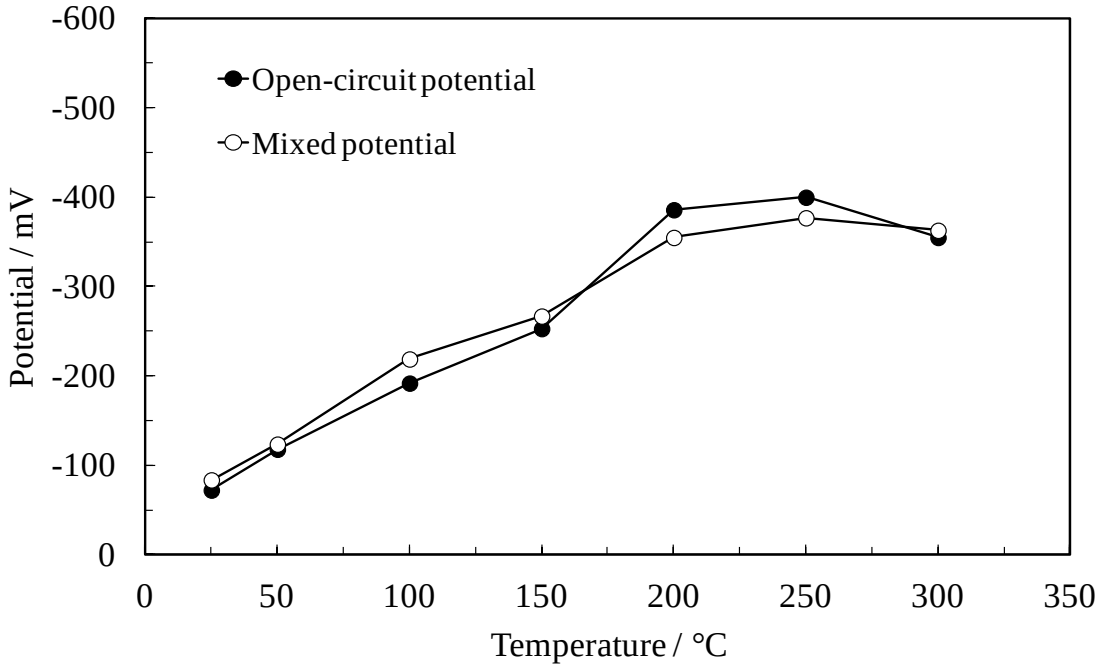

Figure 2-1 Mixed potential estimated from the intersection points of the anodic and cathodic polarization curves and open-circuit potentials of the Pt/C working electrode. The open-circuit potentials were obtained in a mixture of 1000 ppm propane, 3% H_2O, and 5000 ppm O_2[15].

Given on the previous study, the fuel cell electrochemical reactor has the ability to oxidize the propane spontaneously based on the mechanism stated in the scheme 2-1. However, a device like such reactor is difficult to apply to the vehicles, for the small surface are, the large size and the complicated preparation method. Therefore, it is necessary to apply the phenomena in a powder catalyst, which could be used as the washcoat in the commercialized catalytic converters. It would better easily to be made and applied, and considering the cost of the washcoat, the loading amount of the Pt should be as small as possible.

In this study, we would make efforts to develop catalysts with tiny local electrochemical catalyst formed in the interface of the Pt and $Sn_{0.9}In_{0.1}P_2O_7$, as

illustrated in Scheme 2-1(b). The novel catalysts will be compared with the traditional catalysts. To demonstrate the differences between the electrochemical mechanism and the redox mechanism, the $Sn_{0.9}In_{0.1}P_2O_7$ supported metal oxides (MO_x) catalysts were also prepared and tested, because the metals oxides, especially the transition metal oxides, were also commonly referred as active for the hydrocarbon oxidation.

2.2 Experimental Section

2.2.1 Materials and characterization methods

$Sn_{0.9}In_{0.1}P_2O_7$ was prepared using the follow method. SnO_2 and In_2O_3 (Wako) were mixed with 85% H_3PO_4 and ion-exchanged water and held with stirring at 300 °C until a high viscosity paste was formed. This paste was calcined in an alumina pot at 650 °C for 2.5 h and then ground into powder in a mortar.

For catalyst studies, $Pt/Sn_{0.9}In_{0.1}P_2O_7$ (0.01-1.00 wt% Pt contents) catalyst was prepared by impregnation of the surface of the $Sn_{0.9}In_{0.1}P_2O_7$ powder with a Pt precursor ($Pt(NH_3)_4Cl_2 \cdot H_2O$). The $Sn_{0.9}In_{0.1}P_2O_7$ powder was suspended in ion-exchanged water, and an aqueous solution of $Pt(NH_3)_4Cl_2 \cdot H_2O$ was added dropwise to the suspension using micropipettes while stirring at approximately 60 °C. After aging at this temperature overnight, the catalyst powder was oxidized in an air feed at 300 °C for 1 h and then reduced in a 10 vol% H_2 (Ar balance) feed at 450 °C for 1 h. For comparison, a $Pt/\gamma\text{-}Al_2O_3$ (0.01-1.00 wt% Pt) catalyst, which is used as a standard catalyst at Toyota Motor Corporation, was also tested. The $MO_x/Sn_{0.9}In_{0.1}P_2O_7$ catalysts were prepared from their precursor listed in the Table 2-1,

and the loading amount is 5 wt. %. The $Sn_{0.9}In_{0.1}P_2O_7$ powder was suspended in ion-exchanged water, and an aqueous solution of the precursor was added dropwise to at 60 °C. After aging at the temperature overnight, the powders were oxidized in an air feed under the conditions listed in the Table 2-1. To excluding the influence of reduction of the hydrogen, half amounts of the oxidized catalysts were reduced in the same manner with $Pt/Sn_{0.9}In_{0.1}P_2O_7$ catalysts.

2.2.2 Catalyst studies

The activity of the $Pt/Sn_{0.9}In_{0.1}P_2O_7$ catalysts and the $MO_x/Sn_{0.9}In_{0.1}P_2O_7$ catalysts for the HC and NO_x reaction was measured under various conditions. In the case of an ultra-low Pt or $Pt\text{-}Rh/Sn_{0.9}In_{0.1}P_2O_7$ catalyst, a few gram catalyst powders were used as the test sample. Catalytic tests were conducted in a fixed-bed flow reactor. 100 mg catalyst was mixed with 100 mg α-Al_2O_3 in the mortar for a few minutes. Unless otherwise stated, a mixture of 1000 ppm propane, 3% H_2O, and 5000 ppm O_2 in Ar was fed into the reactor, wherein the space velocity (SV) was 9500 h^{-1}. Analysis of the outlet gas was carried out in the same manner as described earlier. All experiments were performed from room temperature to 600 °C. The dispersion state of each component in the catalyst was analyzed using transmission electron microscopy (TEM: JEOL JEM2100F) in conjunction with energy dispersive X-ray (EDX: JEOL JED-2300T) spectroscopy. Specimens for TEM and EDX measurements were prepared by ultrasonic dispersion in *n*-butanol, and a drop of the resultant suspension was evaporated on a Cu grid.

Table 2-1 The list of MOx /$Sn_{0.9}In_{0.1}P_2O_7$ catalysts

M	Precursor	Syn. condition	MO_x
Co	$Co(NO_3)_2$ $6H_2O$	300, 2h	Co_3O_4
V	NH_4VO_3	450, 5h	V_2O_5
Fe	$Fe(NO_3)_3$ $9H_2O$	450, 1h	Fe_2O_3
Mn	$Mn(NO)_2$ $4H_2O$	400, 1h	MnO_2
Ce	$Ce(NO_3)_3$ $6H_2O$	400, 2h	CeO_2
Cu	$Cu(NO_3)_2$ $3H_2O$	450, 1h	CuO
Ag	$AgNO_3$	450, 1h	AgO

2.3 Results and Discussion

2.3.1 $Pt/Sn_{0.9}In_{0.1}P_2O_7$ catalysts

The use of the phenomenon represented in Scheme 1(b) enables propane oxidation at relatively low temperatures, but the reaction area of the electrochemical cell is not sufficiently high to meet the criteria for practical applications. Therefore, we attempted to increase the reaction area for propane reaction by impregnation of the surface of the $Sn_{0.9}In_{0.1}P_2O_7$ support with the Pt metal, wherein the Pt contents were changed from 0.01 to 1.00 wt%. According to the BET tests, the surface area of the $Sn_{0.9}In_{0.1}P_2O_7$ support was 1.0 m^2 g^{-1}. The dispersion of the Pt particles in the $Pt/Sn_{0.9}In_{0.1}P_2O_7$ catalysts was observed by using TEM. From the TEM images in Fig. 2-2, the cluster size of Pt was determined to be approximately 20, 10, and 5 nm at the Pt contents of 1.00, 0.10, and 0.01 wt%, respectively. It is also likely that high dispersion of the metal

on the support surface was accomplished for all the Pt contents tested. The number of active reaction sites was increased.

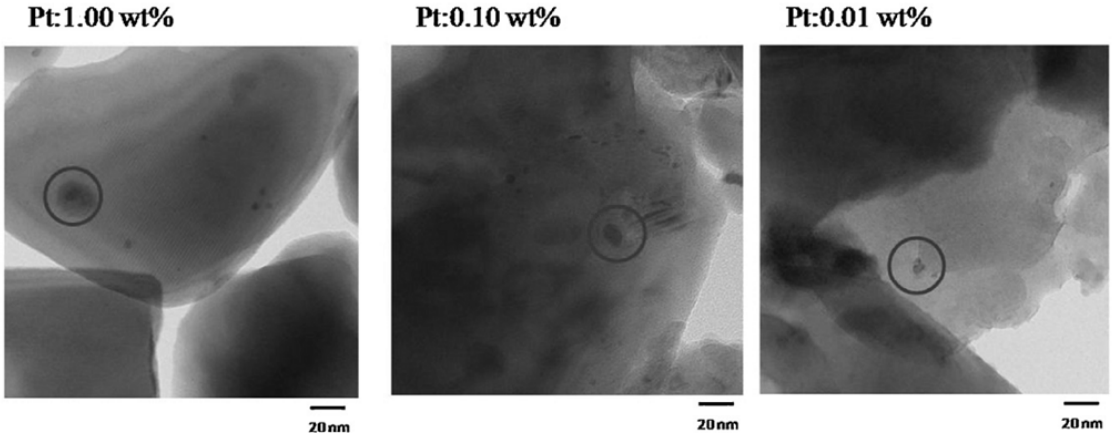

Figure 2-2 TEM characterizations of the $Pt/Sn_{0.9}In_{0.1}P_2O_7$ catalyst with different Pt contents.

The catalytic activity and the effect of varying the Pt content in the $Pt/Sn_{0.9}In_{0.1}P_2O_7$ catalyst on its catalytic activity was investigated using propane oxidation. Figure 2-3 shows the propane conversion as a function of the temperature for the $Pt/Sn_{0.9}In_{0.1}P_2O_7$ catalyst with Pt contents of 0.01, 0.10, and 1.00 wt%. Although the reaction initiation temperature was shifted to higher temperatures by a decrease of the Pt content, the propane conversion reached approximately 90% at 400 °C even for 0.01 wt% Pt.

To further understand the results and compared with the $Pt/\gamma\text{-}Al_2O_3$ catalysts, figure 2-4 shows the temperature at which 50 or 90% conversion was achieved (defined as $T_{50\%}$ or $T_{90\%}$), and data for a $Pt/\gamma\text{-}Al_2O_3$ catalyst with different Pt contents is also shown. $T_{50\%}$ and $T_{90\%}$ for the $Pt/Sn_{0.9}In_{0.1}P_2O_7$ catalyst were lower than those for the $Pt/\gamma\text{-}Al_2O_3$ catalyst at each Pt contents. Interestingly, $T_{50\%}$ and $T_{90\%}$ for the 0.01 wt% $Pt/Sn_{0.9}In_{0.1}P_2O_7$ catalyst were 305 and 380 °C, respectively, which are lower than those for the 0.10 wt% $Pt/\gamma\text{-}Al_2O_3$ catalyst. This means that the use of the $Sn_{0.9}In_{0.1}P_2O_7$ support allows for the reduction of the Pt content by one order of

magnitude or more. The 0.01 wt% Pt/$Sn_{0.9}In_{0.1}P_2O_7$ catalyst was used in subsequent experiments in the chapter 3 and chapter 4.

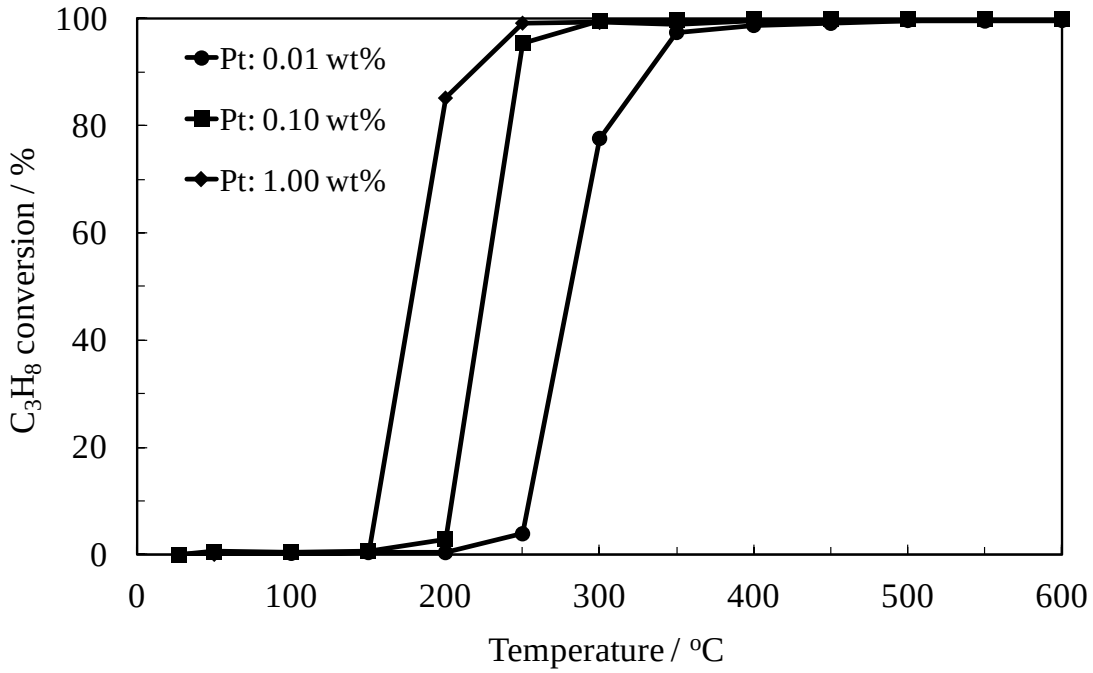

Figure 2-3 Propane conversion over the Pt/$Sn_{0.9}In_{0.1}P_2O_7$ catalysts with different Pt loading contents, 1 wt%, 0.10 wt%, 1.00 wt%. The reactant gas was 1000 ppm propane, 5000 ppm O_2, and 3 vol.% H_2O vapor in Ar.

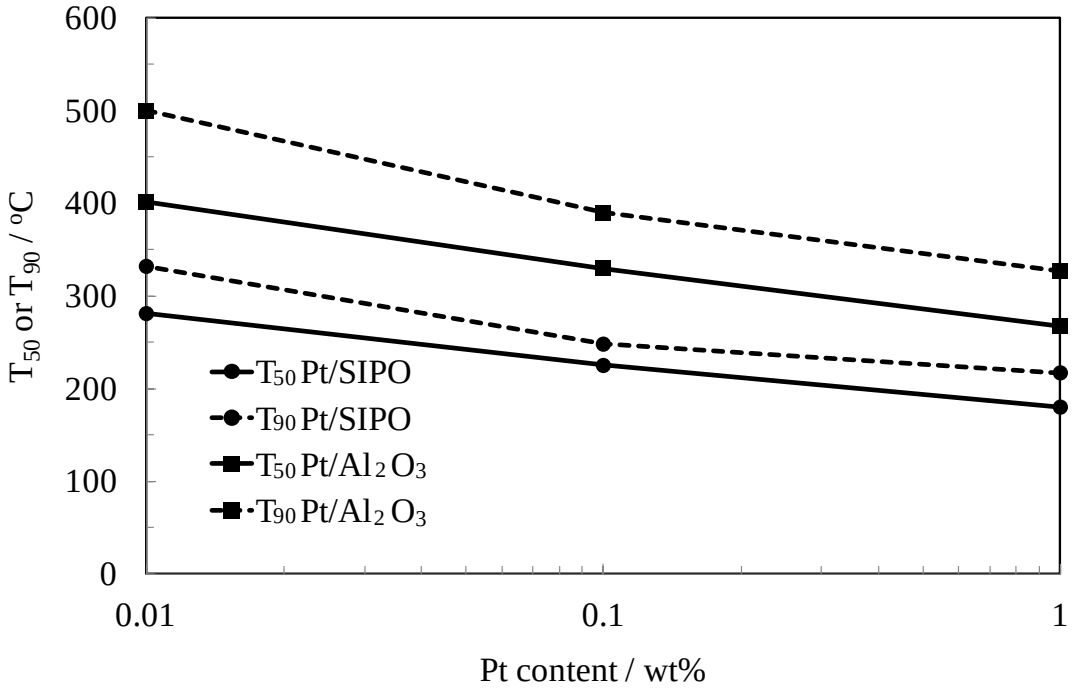

Figure 2-4 $T_{50\%}$ and $T_{90\%}$ for the Pt/SIPO and Pt/γ-Al_2O_3 catalysts

2.3.2 $MO_x/Sn_{0.9}In_{0.1}P_2O_7$ catalysts

The metal oxides with poor electron conductivity were commonly used as the combustion catalysts for the hydrocarbons and a mechanism based on the redox ability of catalysts was usually involved. Thus, the 5 wt. % loading $MO_x/Sn_{0.9}In_{0.1}P_2O_7$ catalysts were prepared to compare with electrochemical catalysts. The compositions of the catalysts were generally identified from the XRD spectra, which were also showed in the Table 2-1. The activity of $MO_x/Sn_{0.9}In_{0.1}P_2O_7$ catalysts was measured using the same manner with the $Pt/Sn_{0.9}In_{0.1}P_2O_7$ catalyst, and the result was plotted in the Figure 2-5. Given the $Pt/Sn_{0.9}In_{0.1}P_2O_7$ catalysts had been reduced by the hydrogen before the reaction, the reduced $MO_x/Sn_{0.9}In_{0.1}P_2O_7$ catalysts were also prepared in the same manner. Compared with the $Pt/Sn_{0.9}In_{0.1}P_2O_7$ catalyst, the conversions for propane over the $MO_x/Sn_{0.9}In_{0.1}P_2O_7$ catalysts were much lower at each temperature,

even with the much larger loading amounts. The supported Co oxides had the lowest initial temperature of 300 ^{o}C and the highest conversion was achieved over the supported Cu oxides at the 600 ^{o}C. After the reduction process, the activity over most of the metal oxides catalysts didn't changed significantly except for the Co oxides, which suggested that the oxidation state of those oxides remained the same when the propane oxidation occurred. The Co oxides catalyst achieved a nearly 80% conversion between 350 and 400 ^{o}C, but reduced sharply at a higher temperature. It can be explained by the reduced oxides would be oxidized again when the temperature increased.

The poor activities of the $MO_x/Sn_{0.9}In_{0.1}P_2O_7$ catalysts indicated that the Pt components cannot be replaced by the metal oxides in the proton conductor supported catalysts. The results could be easily explained by the electrochemical mechanism. The Pt particle in this reaction scheme not only works as the active component but also good conductor of electrons, while the metal oxides are weak electron conductor and can only worked as the normal redox catalysts. Also, even the supported metal oxides were reduced to the metal particles in the hydrogen; they would be oxidized in the air or in the reaction process given their small particle size on the support. The mechanism suggested that we cannot replace the expensive platinum group metals with the metal oxidize to reduce the cost of $Sn_{0.9}In_{0.1}P_2O_7$ supported catalysts, and further confirmed the scheme 2-1.

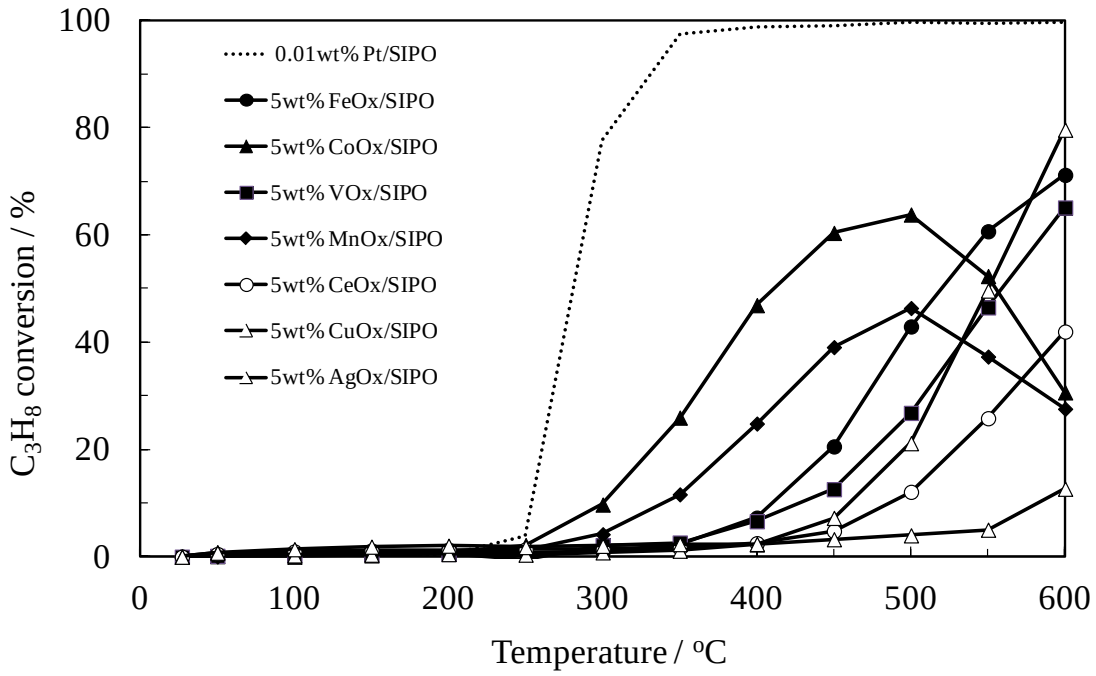

Figure 2-5 Propane conversion over the $MO_x/Sn_{0.9}In_{0.1}P_2O_7$ catalysts. The reactant gas was 1000 ppm propane, 5000 ppm O_2, and 3 vol. % H_2O vapor in Ar.

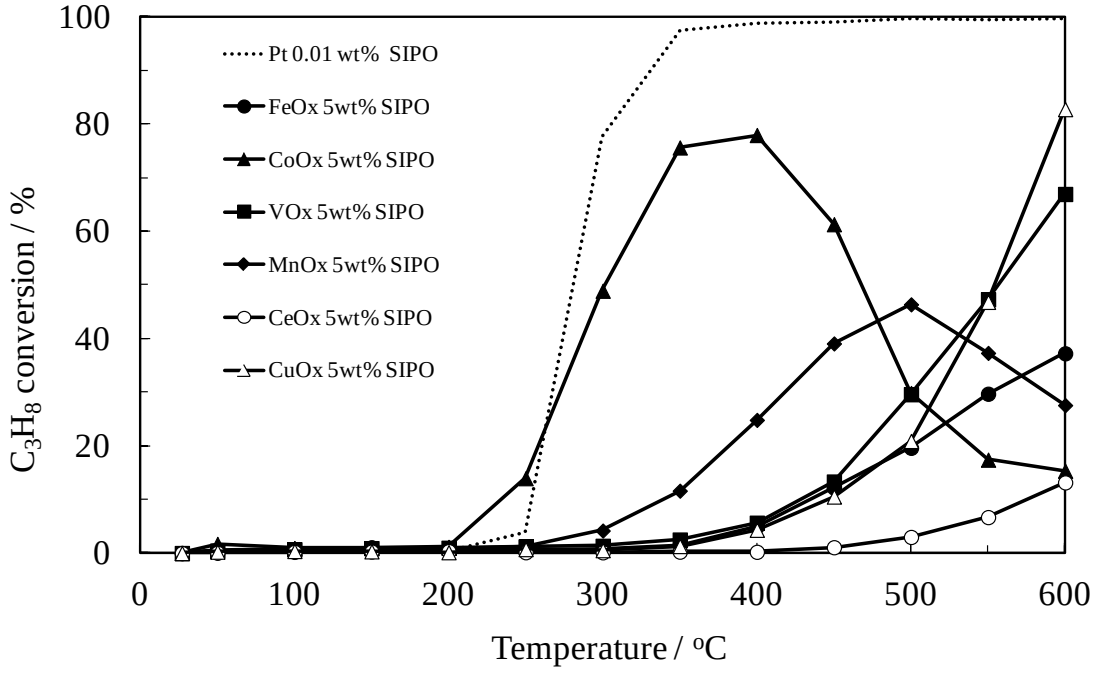

Figure 2-6 Propane conversion over the reduced $MO_x/Sn_{0.9}In_{0.1}P_2O_7$ catalysts. The reactant gas was 1000 ppm propane, 5000 ppm O_2, and 3 vol. % H_2O vapor in Ar.

2.4 Summary

In this study, $Sn_{0.9}In_{0.1}P_2O_7$ and Pt were used as the proton conductor and electrocatalyst, respectively. The electrochemical activation of oxygen also occurred under open-circuit conditions when both H_2O and O_2 were present in the reaction system, which is interpreted as a mixed potential mechanism. This phenomenon was then applied to $Pt/Sn_{0.9}In_{0.1}P_2O_7$ catalysts. Compared with the $Pt/\gamma\text{-}Al_2O_3$ catalysts, $Sn_{0.9}In_{0.1}P_2O_7$ catalysts showed higher catalytic activity at low temperatures and smaller quantities of Pt. The loading amount of Pt was significantly reduced by the impregnating Pt on the $Sn_{0.9}In_{0.1}P_2O_7$, while remaining high activity for propane. The propane conversion reached approximately 90% at 400 °C even for 0.01 wt% Pt. Meanwhile, poor activities of propane over the $MO_x/Sn_{0.9}In_{0.1}P_2O_7$ catalysts further confirmed the electrochemical mechanism. The results shows $Pt/Sn_{0.9}In_{0.1}P_2O_7$ could be a promising solution for the two way catalysis.

2.5 References

[1] J.P.A. Neeft, M. Makkee, and J.A. Moulijn, Diesel particulate emission control, *Fuel Process Technol*. **47**(1), 1-69 (1996).

[2] P. Gelin and M. Primet, Complete oxidation of methane at low temperature over noble metal based catalysts: a review, *Appl Catal B-Environ*. **39**(1), 1-37 (2002).

[3] M.V. Twigg, Progress and future challenges in controlling automotive exhaust gas emissions, *Appl Catal B-Environ*. **70**(1-4), 2-15 (2007).

[4] R. Schneider, D. Kiessling, and G. Wendt, Cordierite monolith supported perovskite-type oxides - catalysts for the total oxidation of chlorinated hydrocarbons, *Appl Catal B-Environ*. **28**(3-4), 187-195 (2000).

[5] T.F. Garetto, E. Rincon, and C.R. Apesteguia, The origin of the enhanced activity of Pt/zeolites for combustion of C-2-C-4 alkanes, *Appl Catal B-Environ*. **73**(1-2),

65-72 (2007).

[6] R. Burch, D.J. Crittle, and M.J. Hayes, C-H bond activation in hydrocarbon oxidation on heterogeneous catalysts, *Catal Today*. **47**(1-4), 229-234 (1999).

[7] T.F. Garetto and C.R. Apesteguia, Oxidative catalytic removal of hydrocarbons over Pt/Al2O3 catalysts, *Catal Today*. **62**(2-3), 189-199 (2000).

[8] J.Y. Luo, M. Meng, J.S. Yao, X.G. Li, Y.Q. Zha, X. Wang, and T.Y. Zhang, One-step synthesis of nanostructured Pd-doped mixed oxides MO_x-CeO_2 (M = Mn, Fe, Co, Ni, Cu) for efficient CO and C3H8 total oxidation, *Appl Catal B-Environ*. **87**(1-2), 92-103 (2009).

[9] Y. Yazawa, H. Yoshida, N. Takagi, S. Komai, A. Satsuma, and T. Hattori, Acid strength of support materials as a factor controlling oxidation state of palladium catalyst for propane combustion, *J Catal*. **187**(1), 15-23 (1999).

[10] B. Grbic, N. Radic, B. Markovic, P. Stefanov, D. Stoychev, and T. Marinova, Influence of manganese oxide on the activity of Pt/Al_2O_3 catalyst for CO and n-hexane oxidation, *Appl Catal B-Environ*. **64**(1-2), 51-56 (2006).

[11] M. Nagao, T. Yoshii, T. Hibino, M. Sano, and A. Tomita, Electrochemical reduction of NOx at intermediate temperatures using a proton-conducting In3+-doped SnP_2O_7 electrolyte, *Electrochem Solid St*. **9**(2), J1-J4 (2006).

[12] P. Heo, K. Ito, A. Tomita, and T. Hibino, A proton-conducting fuel cell operating with hydrocarbon fuels, *Angew Chem Int Edit*. **47**(41), 7841-7844 (2008).

[13] N.M. Markovic and P.N. Ross, Surface science studies of model fuel cell electrocatalysts, *Surf Sci Rep*. **45**(4-6), 121-229 (2002).

[14] W.S. Li, D.S. Lu, J.L. Luo, and K.T. Chuang, Chemicals and energy co-generation from direct hydrocarbons/oxygen proton exchange membrane fuel cell, *J Power Sources*. **145**(2), 376-382 (2005).

[15] K. Tsuneyama, S. Tetanishi, T. Hibino, S. Nagao, H. Hirata, and S. Matsumoto, Low-temperature hydrocarbon combustion over proton conductor/metal-mixed catalysts, *J Catal*. **273**(1), 59-65 (2010).

[16] N. Miura, G.Y. Lu, N. Yamazoe, H. Kurosawa, and M. Hasei, Mixed potential type NOx sensor based on stabilized zirconia and oxide electrode, *J Electrochem Soc*. **143**(2), L33-L35 (1996).

[17] F.H. Garzon, R. Mukundan, and E.L. Brosha, Solid-stale mixed potential gas sensors: theory. experiments and challenges, *Solid State Ionics*. **136** 633-638 (2000).

CHAPTER III

Three Way Catalysis over Pt- and PtRh-$Sn_{0.9}In_{0.1}P_2O_7$ Catalysts

3.1 Introduction

Although the two-way catalysts are still used in many cases, three-way catalysts (TWCs) have been the most widely solution used to purify hydrocarbons (HC), CO, and NO_x in the exhaust of gasoline engines [1-3]. Compared with two-way catalysts used to oxidize hydrocarbons, in the so-called three-way catalysts, unburned hydrocarbons (HCs) and carbon monoxide (CO) are oxidized, and at the same time, produced nitrogen oxides (NOx) are reduced, which is accomplished by controlling the air/fuel ratio of the exhaust close to a stoichiometric value of 14.6.

The TWCs promote the following reactions for CO, HC, and NO_x in the exhaust [4]:

$$CO + 1/2O_2 \rightarrow CO_2 \quad (1)$$

$$CO + H_2O \rightarrow CO_2 + H_2 \quad (2)$$

$$C_mH_n + (1 + n/4)O_2 \rightarrow mCO_2 + n/2H_2O \quad (3)$$

$$NO(\text{or } NO_2) + H_2 \rightarrow 1/2N_2 + H_2O \quad (4)$$

$$(2 + n/2)NO(\text{or } NO_2) + C_nH_m \rightarrow (1 + n/4)N_2 + mCO_2 + n/2H_2O \quad (5)$$

Typically, the CO reaction first begins, followed by the HC and NO_x reaction. Therefore, the ability of TWCs is determined by the catalytic activity for the HC and

NO_x reaction. The activation of C-H bonds in HC is considered to be the key initial step in the HC oxidation. There seems to be little doubt regarding the role of chemisorbed or combined oxygen species (so-called active oxygen) in the extraction of hydrogen from the C-H bond in HC [5, 6].

As we stated in chapter 2, the activation of propane is generally catalyzed on the Pt catalysts, and Rh is used to improve the conversion of NO. However, the commonly used Pt and Rh catalysts are very expensive, and Pt and Rh sources are unevenly distributed in the world, which raise the cost of automotive converters production, since catalyst coating technology leverages up to almost 90% of total catalytic converter costs. In order to solve this problem, one approach is to use Pd as the only active metal in TWCs, which has been aggressively pursued over the past decade, but the commercialization of this system has not yet been realized [7-13]. An alternative approach is to reduce the Pt and Rh contents while maintaining high catalytic activity. Papavasiliou et al. decreased the Pt content to 0.5 wt% over γ-Al_2O_3 by using $Ce_{0.4}Zr_{0.5}La_{0.1}O_{1.9}$ as a promoter [14]. It is believed that a further reduction in these precious metals would enhance the position of TWCs as preferred emission control technologies. Another factor is that researcher find the loading amount is strongly related with the light-off temperature of the catalysts. In the other word, low Pt and Rh loading contents will increase the light–off temperature of the catalysts. However, the regulations in today have been tensed so much that even the emissions during the cold-start transients have to be removed to meet the requirements. A majority of hydrocarbon (60%–80% of the total emitted) are produced in the cold start portion of the automobile, according to SAE (Society of Automotive Engineer, SAE. 961954). However, the temperature of the exhaust from the cold-start transient is usually around

200 ^{o}C, which is much lower than the temperature of 300-500 ^{o}C required by the normally two way catalysts. In fact, there is tendency to increase the loading amount of precious metals order to meet regulations, especially for the diesel engine. Therefore, it is important for our catalysts to maintain the catalysts activity in a relatively low range while decrease the loading contents of precious metals.

Also from the discussion of Chapter 2, it can be find that H_2O could dissociate into protons, electrons, and active oxygen species are generated at a Pt/C anode in an electrochemical reactor Pt/C|$Sn_{0.9}In_{0.1}P_2O_7$|Pt/C, leading to oxidation of propane to CO_2 [15, 16].

$$C_3H_8 + 6H_2O \rightarrow 3CO_2 + 20H^+ + 20e^- \quad (6)$$

On the other hand, NO_x is dissociated into $N_{(ad)}$ and $O_{(ad)}$ on the surface of Pt, promoted by previously adsorbed $H_{(ad)}$ [17]. We also recently reported that NO reacted with protons and electrons to form N_2 and H_2O at a Pt/C cathode in the same electrochemical cell as described above [18, 19].

$$NO + 2H^+ + 2e^- \rightarrow 1/2N_2 + H_2O \quad (7)$$

More importantly, propane oxidation and NO reduction proceeded according to Eqs. (6) and (7), respectively, at temperatures at 200 °C or lower, which suggests that high activities of the Pt catalyst for these reactions are achieved even at reduced Pt contents.

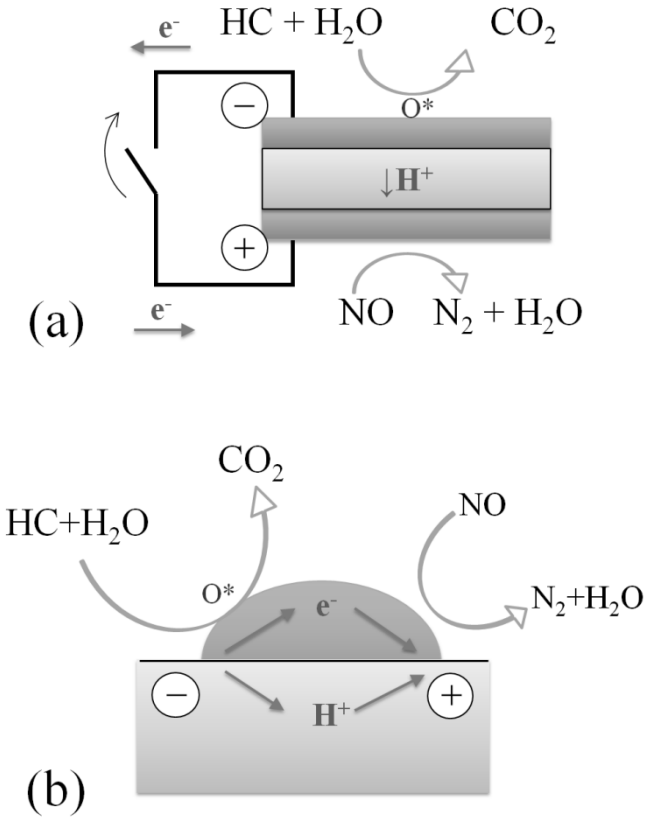

Scheme 3-1.Reaction scheme for propane oxidation and NO reduction in (a) a fuel cell and (b) local electrochemical cell.

Based on these observations, it is expected that an electrochemical reactor for the HC and NO_x reaction can be developed through the reactions shown in Eqs. (6) and (7) by short-circuiting the reactor, as illustrated in Scheme 1(a). Moreover, if nanoscale electrochemical reactors can be successfully produced by impregnating $Sn_{0.9}In_{0.1}P_2O_7$ with Pt, then the reaction area for the HC and NO_x reaction can be drastically increased, as illustrated in Scheme 3-1(b). Therefore, we are looking forward to inspect the HC and NO_x reaction through Eqs. (6) and (7) by using an electrochemical cell with the Pt/C anode and cathode, and demonstrate the advantage of using nano-scale electrochemical reactors with ultra-low Pt loadings for the HC and NO_x reaction. Then

we will attempt to add the promising promoter Rh to the $Pt/Sn_{0.9}In_{0.1}P_2O_7$ catalyst to enhance the NO activity.

3.2 Experimental Section

3.2.1 Materials and characterization methods

$Sn_{0.9}In_{0.1}P_2O_7$ was prepared in the same manner with Chapter 2. Briefly, SnO_2 and In_2O_3 (Wako) were mixed with 85% H_3PO_4 and ion-exchanged water and held with stirring at 300 °C until a high viscosity paste was formed. This paste was calcined in an alumina pot at 650 °C for 2.5 h and then ground in a mortar. The BET surface area of $Sn_{0.9}In_{0.1}P_2O_7$ was measured using a Micromeritics automated system. All samples were degassed under vacuum at 100 °C for 1 h and then 250 °C for 3 h prior to BET surface area measurements.

For electrochemical cell studies, the $Sn_{0.9}In_{0.1}P_2O_7$ powder was uniaxially pressed into pellets (12 mm diameter, ca. 1.0 mm thick) under a pressure of 200 MPa and used as the electrolyte. A Pt/C (10 wt% Pt/C, 0.6 mg Pt cm^{-2}) electrode with a gas diffusion layer was purchased from BASF. For catalyst studies, $Pt/Sn_{0.9}In_{0.1}P_2O_7$ (0.01 wt% Pt contents) and $Pt\text{-}Rh/Sn_{0.9}In_{0.1}P_2O_7$ catalysts (0.01 wt% Pt content and 0.0025-0.0100 wt% Rh contents) were prepared by impregnation of the surface of the $Sn_{0.9}In_{0.1}P_2O_7$ powder with a Pt precursor ($Pt(NH_3)_4Cl_2 \cdot H_2O$) and a Rh precursor ($(NH_4)_3RhCl_6 \cdot H_2O$). The $Sn_{0.9}In_{0.1}P_2O_7$ powder was suspended in ion-exchanged water, and an aqueous solution of $Pt(NH_3)_4Cl_2 \cdot H_2O$ or two aqueous solutions of $Pt(NH_3)_4Cl_2 \cdot H_2O$ and $(NH_4)_3RhCl_6 \cdot H_2O$ were added dropwise to the suspension using

micropipettes while stirring at approximately 60 °C. After aging at this temperature overnight, the catalyst powder was oxidized in an air feed at 300 °C for 1 h and then reduced in a 10 vol% H_2 (Ar balance) feed at 450 °C for 1 h. The dispersion state of each component in the catalyst was analyzed using transmission electron microscopy (TEM) in conjunction with energy dispersive X-ray (EDX) spectroscopy. For comparison with the $Pt/Sn_{0.9}In_{0.1}P_2O_7$ catalyst, a Pt/γ-Al_2O_3 (0.01-1.00 wt% Pt) catalyst, which is used as a standard catalyst at Toyota Motor Corporation, was also tested.

3.2.2 Electrochemical cell studies

The reactions shown in Eqs. (6) and (7) were investigated using an electrochemical cell. The two Pt/C electrodes (area: 0.5 cm^2) were attached on opposite sides of the electrolyte. In both cases, an Au mesh was employed as a current collector. Two electrode chambers were set up by placing the cell assembly between two alumina tubes, as illustrated in Fig. 3-1(a). A mixture of 1000 ppm propane and 3 vol% H_2O in Ar was supplied to the anode at a flow rate of 30 mL min^{-1}, and 1000 ppm NO diluted with Ar was supplied to the cathode at a flow rate of 30 mL min^{-1}. The current was applied with a Hokuto Denko HA-501 galvanostat. The concentrations of propane, CO_x (CO_2 and CO), and O_2 in the outlet gas from the anode chamber were analyzed using an on-line Varian CP-4900 gas chromatograph, and the concentration of NO_x (NO and NO_2) in the outlet gas from the cathode chamber were monitored using an on-line Horiba PG-225 NO_x gas analyzer. Propane oxidation and NO reduction were also evaluated using a half-cell with the Pt/C electrode, as illustrated in Fig. 3-1(b). Besides $Sn_{0.9}In_{0.1}P_2O_7$, silica and yttria-stabilized zirconia (YSZ) pellets were also used as the electrolytes in

the half-cell. The electrode was supplied with a mixture of 1000 ppm propane, 1000 ppm NO, and 3 vol% H_2O vapor in Ar at a flow rate of 30 mL min^{-1}. Analysis of the outlet gas was conducted as described above.

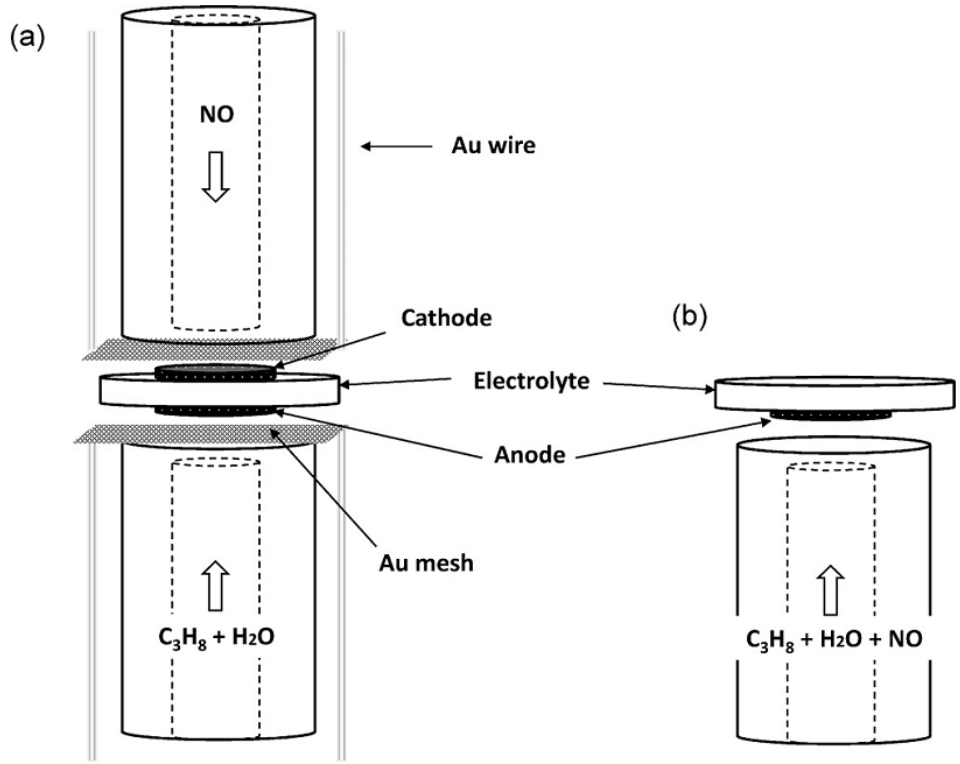

Figure 3-1 Illustrations of the electrochemical cell (a) and the half-cell (b).

3.2.3. Catalyst studies

The activity of the Pt or Pt-Rh/$Sn_{0.9}In_{0.1}P_2O_7$ catalyst for the HC and NO_x reaction was measured under various conditions. The number of reaction sites on the Pt or Pt-Rh surface was measured by the CO pulse method at room temperature. In the case of an ultra-low Pt or Pt-Rh/$Sn_{0.9}In_{0.1}P_2O_7$ catalyst, a few gram catalyst powder was used as the test sample. Catalytic tests were conducted in a fixed-bed flow reactor. 100 mg catalyst was mixed with 100 mg α-Al_2O_3 in the mortar for a few minutes. Unless otherwise stated, a mixture of 1000 ppm propane, 1000 ppm NO, 3% H_2O, and 4500

ppm O_2 in Ar was fed into the reactor, wherein the space velocity (SV) was 9500 h^{-1}. Analysis of the outlet gas was carried out in the same manner as described earlier. All experiments were performed from room temperature to 600 °C.

3.3 Results and Discussion

3.3.1. Electrochemical testing of Scheme 3-1

Propane oxidation and NO reduction represented in Scheme 1(a) were first investigated using the electrochemical cell, in which the N_2 was applied in the cathode instead of O_2. It is necessary for the realization of Scheme 1(a) to generate a large electromotive force (EMF) and short-circuit current from the electrochemical cell, even if the propane and NO concentrations are at ppm levels. The current density-cell voltage curves were measured in the temperature range from 50 to 250 ºC. Figure 3-2 shows that both the EMF and short-circuit current increased with temperature. The resultant EMF and short-circuit current reached 298 mV and >9 mA cm^{-2}, respectively, at 250 ºC. This result suggests the possibility of a fuel-cell type of reactor capable of operating at low propane and NO concentrations.

Analysis of the outlet gases from the two electrode chambers provides evidence for the above suggestion. Figure 3-3 shows that both propane oxidation and NO reduction did not occur under open-circuit conditions, whereas the conversions of these gases were increased by discharging the electrochemical cell, wherein almost linear relationships between the conversion and the current density were obtained. For the anode wherein a mixture of propane and H_2O were fed, the formation of CO_2 was

observed, and the CO_2 concentration at each current density was well in agreement with the theoretical value calculated from Faraday's law based on a twenty-electron reaction corresponding to Eq. (6). This is indicative that propane oxidation proceeded as in Eq. (6). For the cathode wherein NO diluted with Ar was fed, we did not analyze the product. However, it seems that N_2O rather than N_2 are converted from NO, because Fig. 3 shows that the NO conversion at each current density was higher than the value predicted from the propane conversion: since Eq. (7) is a two-electron reaction, the NO conversion should always be ten times as much as the propane conversion, however, it actually accounted for approximately twenty times compared to the propane conversion. Thus, the following one-electron reaction is concluded to be predominant at least under the present conditions:

$$NO + H^+ + e^- \rightarrow 1/2N_2O + 1/2H_2O \quad (8)$$

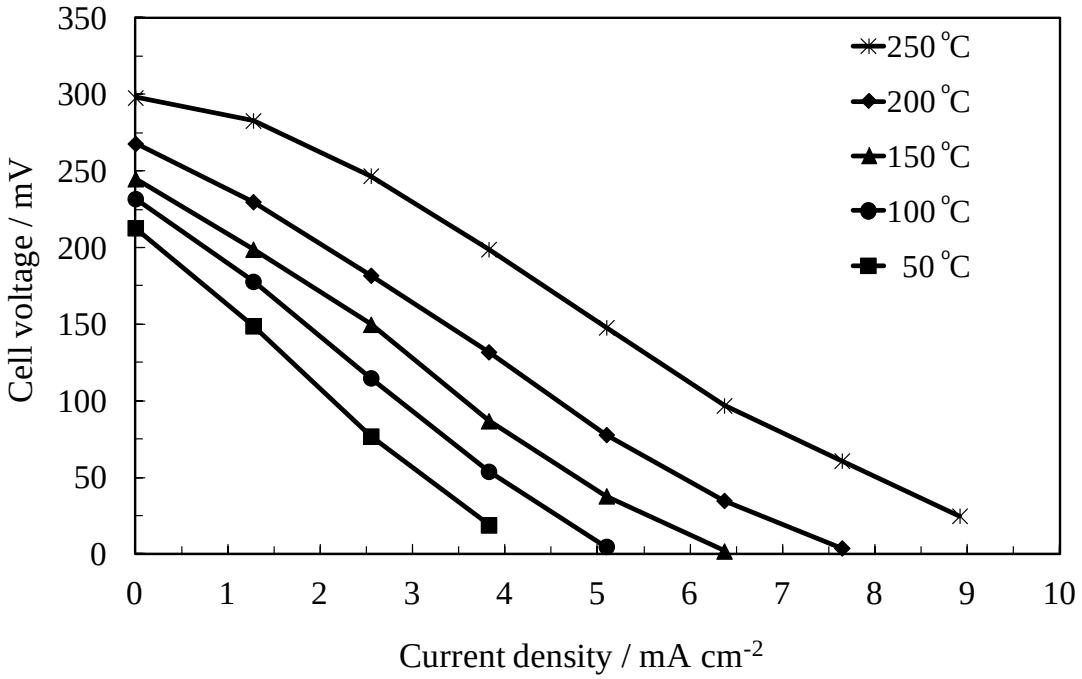

Figure 3-2 Cell performance characteristics from 50 to 250 ℃. A mixture of 1000 ppm propane and 3 vol.% H_2O in Ar was supplied to the anode, and 1000 ppm NO diluted

with Ar was supplied to the cathode.

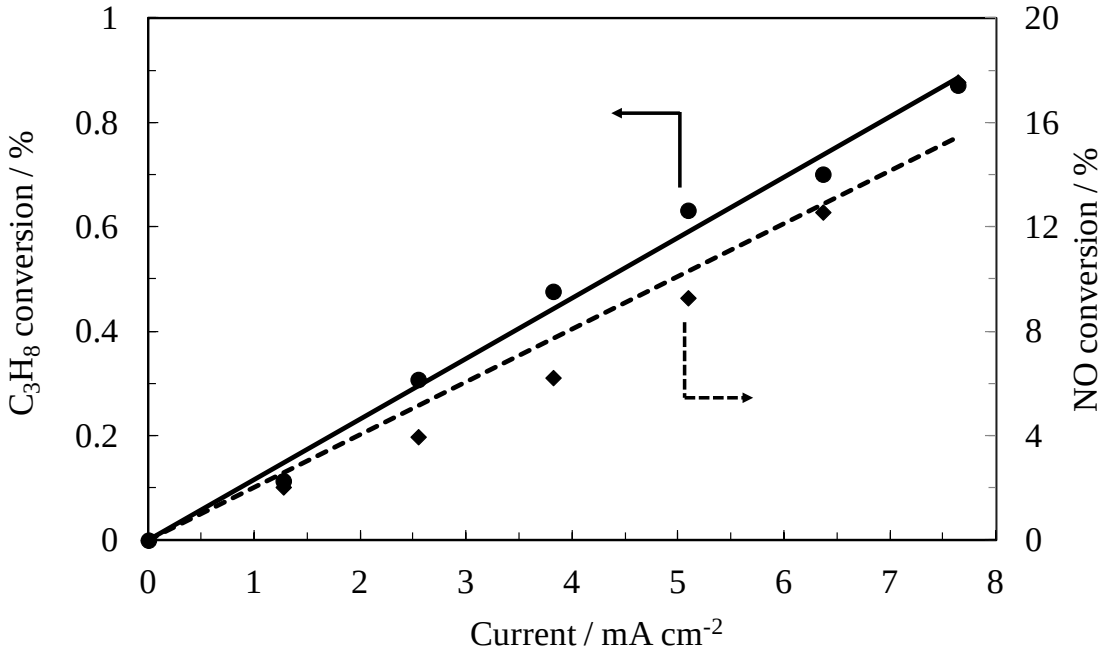

Figure 3-3 Propane and NO conversions over the Pt/C electrodes during cell discharge at 250 °C. A mixture of 1000 ppm propane and 3 vol.% H_2O in Ar was supplied to the anode, and 1000 ppm NO diluted with Ar was supplied to the cathode.

It is believed that both anodic and cathodic sites are present on the same electrode surface due to its heterogeneity at the atomic level [20-22]. If propane, H_2O, and NO coexist in the reaction system, this structure enables the formation of a local electrochemical cell at the electrode-electrolyte interface. Since the electrode also functions as a lead wire, the local electrochemical cell would then be short-circuited. Consequently, propane would react with NO through the reactions shown in Eqs. (6) and (8) even in the half-cell, as displayed in Scheme 1(b). We next prove this scheme by measuring the catalytic activity of the Pt/C electrode for propane oxidation and NO reduction using various electrolytes. Plots of the propane and NO conversions as a function of the temperature are shown in Figure 3-4. By comparing the results for $Sn_{0.9}In_{0.1}P_2O_7$ with those for silica and YSZ, it can be seen that the use of

$Sn_{0.9}In_{0.1}P_2O_7$ significantly enhanced the propane and NO conversions, especially at temperatures above 150 °C. Note that under the present conditions, $Sn_{0.9}In_{0.1}P_2O_7$ shows proton conductivities above 0.1 S cm^{-1}, whereas the other two electrolytes show extremely low ion conductivities (10^{-6}~10^{-4} S cm^{-1}) [18]. This supports the validity of Scheme 1(b), although a non-electrochemical reaction between propane and NO proceeds to some extent. It is thought that the differences in propane and NO conversions between the half-cells with the $Sn_{0.9}In_{0.1}P_2O_7$ and silica or YSZ electrolytes correspond to the propane and NO conversions based on the electrochemical reactions. Another important result is that the propane and NO conversions were almost zero % at all over a Pt-free electrode, which means that the Pt catalyst plays an important role in the propane and NO reaction. In other words, $Sn_{0.9}In_{0.1}P_2O_7$ itself has no catalytic activity for this reaction.

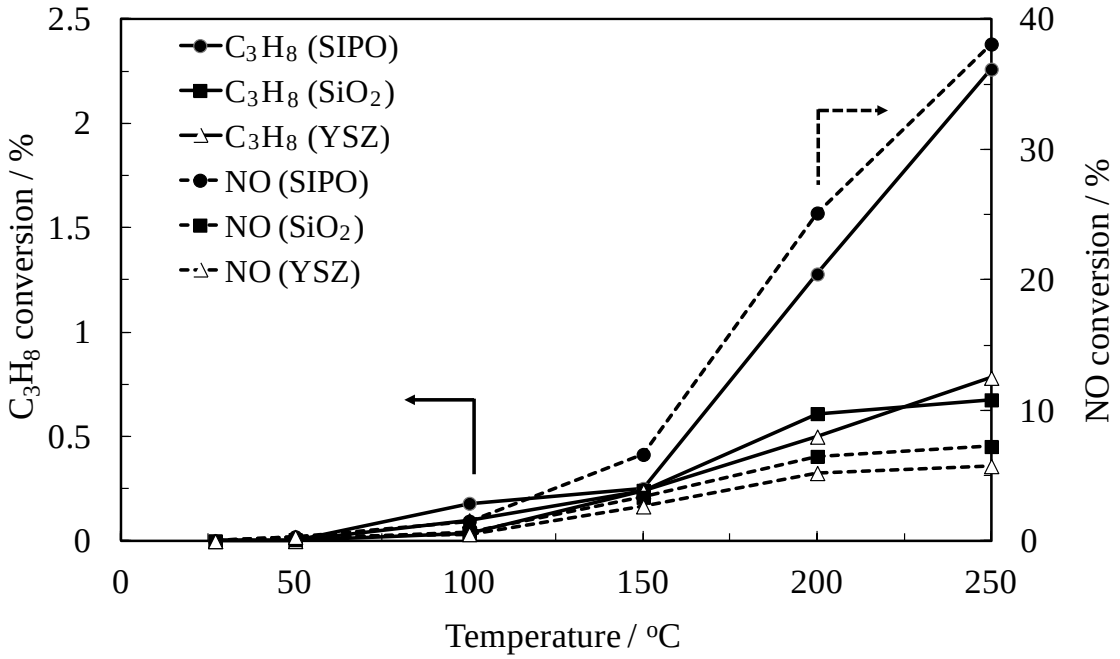

Figure 3-4 Plots of propane and NO conversions as a function of temperature using $Sn_{0.9}In_{0.1}P_2O_7$, silica, and YSZ as electrolyte substrates. The reactant gas was 1000 ppm propane, 1000 ppm NO, and 3 vol% H_2O vapor in Ar.

3.3.2. Propane oxidation and NO reduction over a $Pt/Sn_{0.9}In_{0.1}P_2O_7$

The activity of the $Pt/Sn_{0.9}In_{0.1}P_2O_7$ catalyst for propane oxidation and NO reduction was then measured in a mixture feed of propane, H_2O, NO, and O_2 in Ar. The results are shown in Fig. 3-5 along with the data for the 0.01 wt% $Pt/\gamma\text{-}Al_2O_3$ catalyst. The $Pt/Sn_{0.9}In_{0.1}P_2O_7$ catalyst exhibited ignition temperatures of 250 °C for propane oxidation and of 300 °C for NO reduction, which are much lower than the corresponding ignition temperatures for the $Pt/\gamma\text{-}Al_2O_3$ catalyst. Even larger differences were observed in $T_{50\%}$: $T_{50\%}$ was 310 °C for propane oxidation over the $Pt/Sn_{0.9}In_{0.1}P_2O_7$ catalyst, 385 °C for NO reduction over the $Pt/Sn_{0.9}In_{0.1}P_2O_7$ catalyst, 430 °C for propane oxidation over the $Pt/\gamma\text{-}Al_2O_3$ catalyst, and 535 °C for NO reduction over the $Pt/\gamma\text{-}Al_2O_3$ catalyst.

Comparison of the turnover frequency (TOF) for the above catalysts is useful to evaluate in more detail their differences in catalytic activity. The temperature dependence of the TOF for Pt in the above catalysts is shown in Figure 3-6. The number of reaction sites on the Pt surface was measured by the CO pulse method at room temperature. For both propane oxidation and NO reduction, the TOF values of the $Pt/Sn_{0.9}In_{0.1}P_2O_7$ catalyst were found to be three or four orders of magnitude higher than those of the $Pt/\gamma\text{-}Al_2O_3$ catalyst. The results indicated that $Pt/Sn_{0.9}In_{0.1}P_2O_7$ catalyst has a higher activity for propane oxidation. Moreover, the $Pt/Sn_{0.9}In_{0.1}P_2O_7$ catalyst exhibited considerably lower activation energies (73 kJ mol^{-1} for propane oxidation and 89 kJ mol^{-1} for NO reduction), compared to the $Pt/\gamma\text{-}Al_2O_3$ catalyst (182 kJ mol^{-1} for propane oxidation and 191 kJ mol^{-1} for NO reduction). Therefore, it is

concluded that there is a large difference in the reaction mechanism for the propane and NO reaction between the two catalysts. This can be explained by the assumption that propane oxidation and NO reduction over the $Pt/Sn_{0.9}In_{0.1}P_2O_7$ catalyst proceed through the electrochemical reactions shown in Eqs. (6) and (8) (or (7)), respectively. Meanwhile, the non-electrochemical reaction shown in Eq. (5) is a main pathway over the $Pt/\gamma\text{-}Al_2O_3$ catalyst.

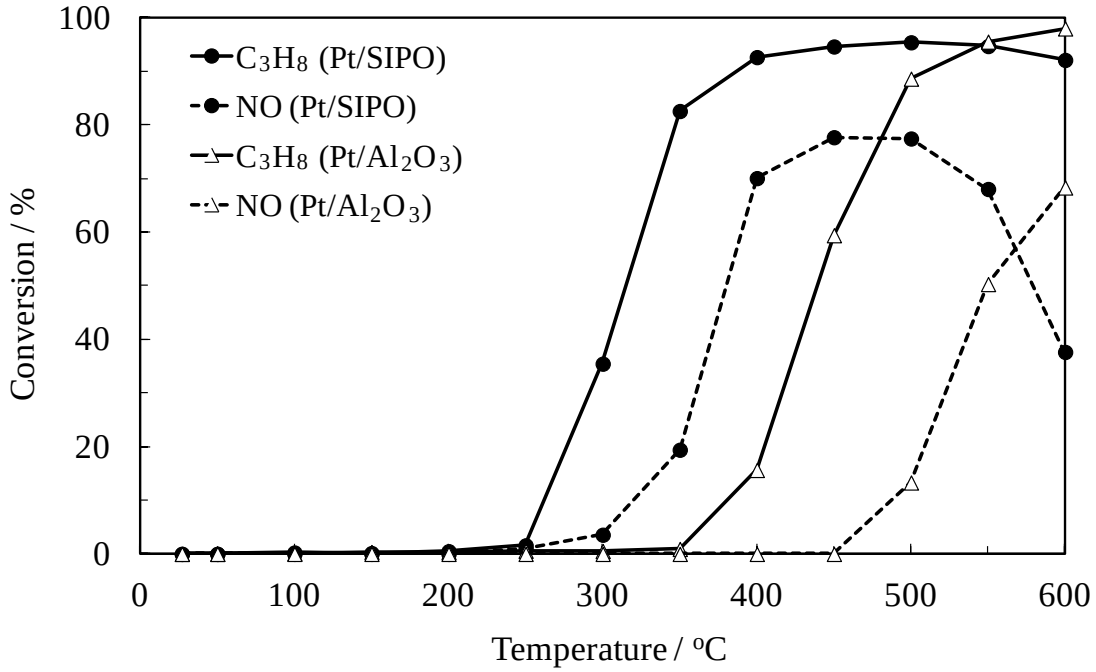

Figure 3-5 Plots of propane and NO conversions as a function of temperature for the 0.01 wt% $Pt/Sn_{0.9}In_{0.1}P_2O_7$ and 0.01 wt% $Pt/\gamma\text{-}Al_2O_3$ catalysts. The reactant gas was 1000 ppm propane, 1000 ppm NO, 4500 ppm O_2, and 3 vol% H_2O vapor in Ar.

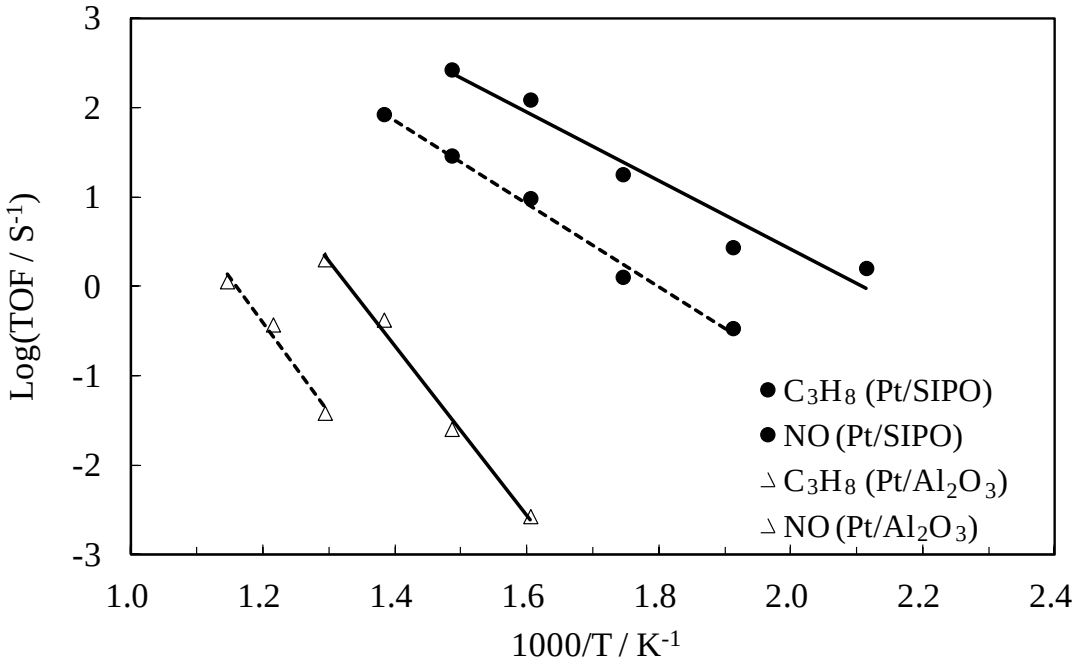

Figure 3-6 Plots of TOFs for propane oxidation and NO reduction as a temperature for the 0.01 wt% $Pt/Sn_{0.9}In_{0.1}P_2O_7$ and 0.01 wt% $Pt/\gamma\text{-}Al_2O_3$ catalysts.

3.3.3. Propane oxidation and NO reduction over a Pt-Rh/$Sn_{0.9}In_{0.1}P_2O_7$

Although the $Pt/Sn_{0.9}In_{0.1}P_2O_7$ catalyst showed a higher catalytic activity for propane oxidation and NO reduction compared to the $Pt/\gamma\text{-}Al_2O_3$ catalyst, the NO conversion over the $Pt/Sn_{0.9}In_{0.1}P_2O_7$ catalyst was drastically reduced above 500 ℃ (Fig. 3-5). This is not due to the deterioration of the $Pt/Sn_{0.9}In_{0.1}P_2O_7$ catalyst, because NO reduction was almost reversible in the temperature range from 500 to 600 ℃. Probably, the reaction shown in Eq. (8) (or (7)) competes with the following oxygen reduction reaction under such conditions:

$$O_2 + 4H^+ + 4e^- \rightarrow 2H_2O \qquad (9)$$

This causes a decrease in the current efficiency for NO reduction at the cathodic site in

the local electrochemical cell. A similar competition reaction was reported for electrochemical reactors [23].

It is well established that Rh promotes the dissociative adsorption of NO, enhancing NO reduction [24]. Therefore, an attempt was made to increase the catalytic activity for NO reduction by the addition of Rh to Pt. Through trial and error, NO reduction over the Pt-Rh/$Sn_{0.9}In_{0.1}P_2O_7$ catalyst was the most significant at a Rh content of 0.005%. The TEM image of this catalyst reveals that the cluster size of Pt-Rh was approximately 10 nm (Fig. 3-7), which is slightly larger than that of Pt in the 0.01 wt% Pt/$Sn_{0.9}In_{0.1}P_2O_7$ catalyst. In addition, the EDX spectrum of Pt-Rh cluster shows that the composition of the cluster was in agreement with that of source materials in the preparation within experimental error (Table. 3-1).

The activity of the Pt-Rh/$Sn_{0.9}In_{0.1}P_2O_7$ catalyst for propane oxidation and NO reduction is shown in Fig. 3-8, in addition to the data for the Pt/$Sn_{0.9}In_{0.1}P_2O_7$ catalyst. Regardless of the growth of the Pt-Rh cluster, the NO conversion over the Pt-Rh/$Sn_{0.9}In_{0.1}P_2O_7$ catalyst was higher than that over the Pt/$Sn_{0.9}In_{0.1}P_2O_7$ catalyst at all the temperatures tested. It should be emphasized that $T_{50\%}$ for NO reduction over the Pt-Rh/$Sn_{0.9}In_{0.1}P_2O_7$ catalyst was successfully reduced to 355 °C. Similarly, an increase in the propane conversion was observed, although the extent was not large. These effects are attributable to either the electrochemical enhancement for the reactions shown in Eqs. (6) and (8) (or (7)) or to non-electrochemical enhancement for the reaction shown in Eq. (5).

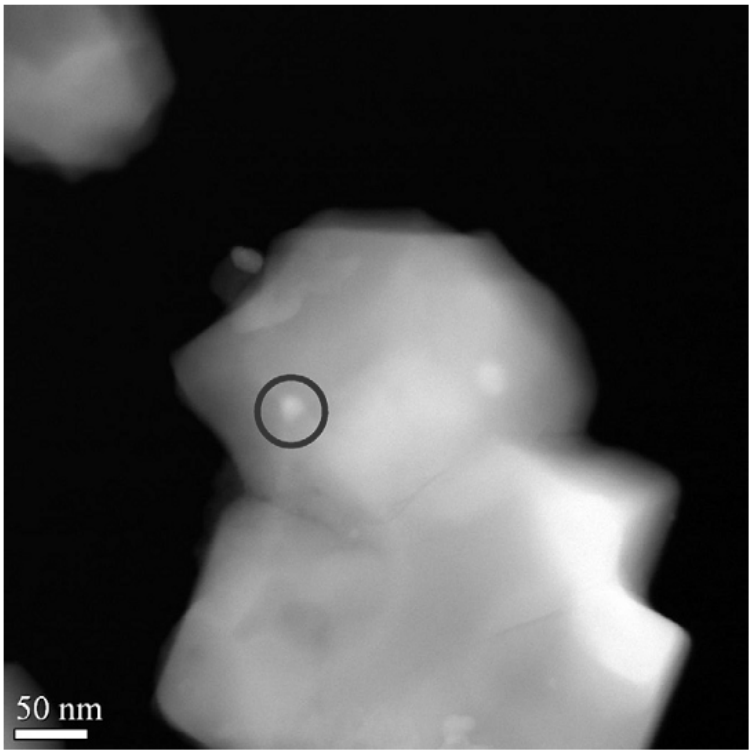

Figure 3-7 TEM and EDX characterizations of the Pt-Rh/$Sn_{0.9}In_{0.1}P_2O_7$ catalyst. The Pt and Rh contents were 0.01 and 0.005 wt%, respectively.

Table 3-1 Composition of PtRh/SIPO catalyst determined by EDX.

Element	keV	wt.%	S.D.	at.%
O	0.53	31.02	0	64.13
P	2.01	22.62	0.01	24.16
Rh	2.7	2.18	0.21	0.7
Sn	3.44	32.24	0.01	8.98
Pt	9.44	11.94	0.06	2.02

S.D., standard deviation.

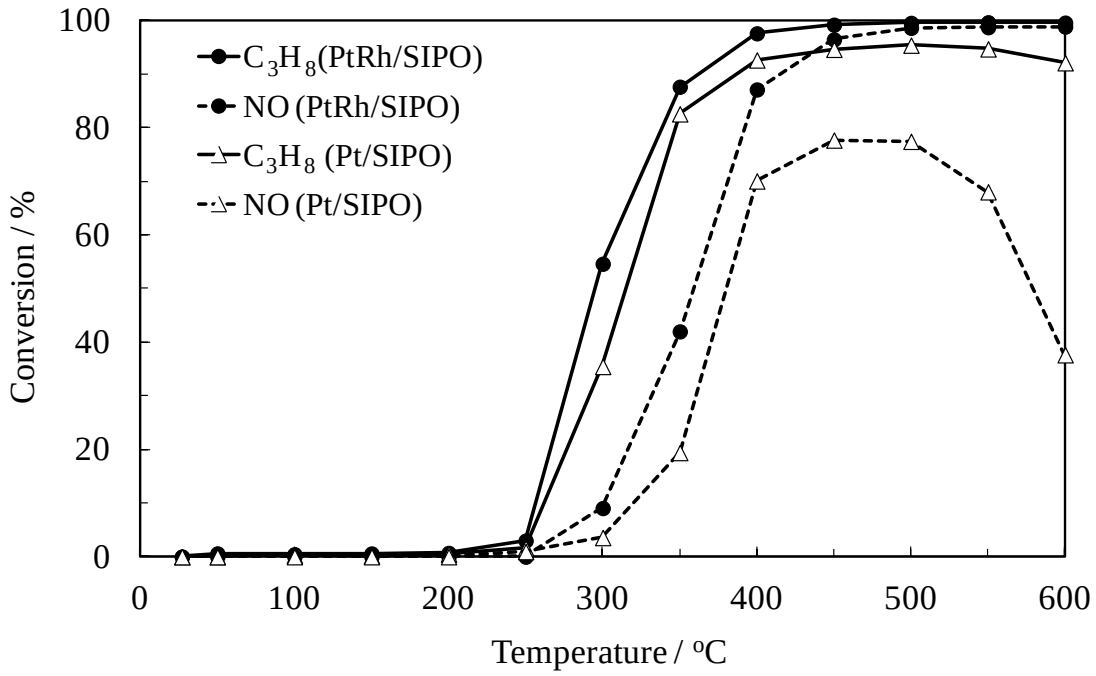

Figure 3-8 Propane and NO conversions as a function of temperature for the Pt/SIPO (0.01 wt.% Pt) and Pt–Rh/SIPO (0.01 wt.% Pt, 0.005 wt.% Rh) catalysts. The reactant gas was 1000 ppm propane, 1000 ppm NO, 4500 ppm O_2, and 3 vol.% H_2O vapor in Ar.

In order to gain more detailed insights into the above results, the TOF values of the Pt-Rh/$Sn_{0.9}In_{0.1}P_2O_7$ catalyst for propane oxidation and NO reduction were compared with those of Pt/$Sn_{0.9}In_{0.1}P_2O_7$ catalyst. As shown in Figure 3-9, the addition of Rh to Pt enhanced the TOF values for propane oxidation and especially NO reduction. However, the activation energies of the Pt-Rh/$Sn_{0.9}In_{0.1}P_2O_7$ catalyst for the two reactions were near those of the Pt/$Sn_{0.9}In_{0.1}P_2O_7$ catalyst, which strongly suggests a similarity in the reaction pathway over the two catalysts. It is thus reasonable that the added Rh promotes the reactions shown in Eqs. (6) and (8) (or (7)) rather than the reaction shown in Eq. (5).

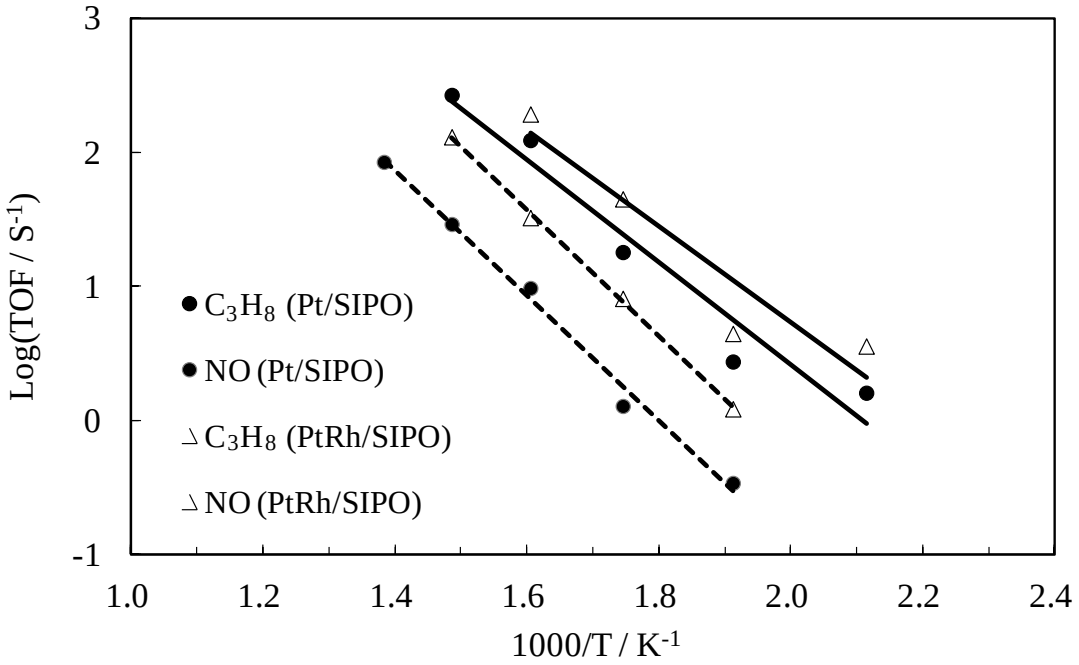

Figure 3-9 Plots of TOFs for propane oxidation and NO reduction as a function of temperature for the Pt/SIPO (0.01 wt.% Pt) and Pt–Rh/SIPO (0.01 wt.% Pt, 0.005 wt.% Rh) catalysts.

3.3.4. Propane and NO reaction under various conditions

Finally, we evaluated the other characteristics of the Pt-Rh/$Sn_{0.9}In_{0.1}P_2O_7$ catalyst for propane oxidation and NO reduction. All the experiments in the previous sections were conducted wherein the ratio between the available oxygen and the oxygen needed for full conversion to CO_2, H_2O, and N_2 (defined as S) was stoichiometry. Here, the S value is written using the O_2, propane, and NO concentrations as below [12].

$$S = (2[O_2] + [NO])/10[C_3H_8] \quad (10)$$

The dependence of the S value on the activity of the Pt-Rh/$Sn_{0.9}In_{0.1}P_2O_7$ catalyst for the propane and NO reaction was investigated by adjusting the O_2 concentration at 450 °C. It can be seen from Figure 3-10 that while NO reduction was rapidly degraded at S > 1, propane oxidation proceeded over a wide S range. The latter behavior may be

explained by a redox activity for $Sn_{0.9}In_{0.1}P_2O_7$. Not only protons, $H_i^{\cdot}$, but also oxygen vacancies, Vö, have been reported as possible compensating defects in this material [25].

$$[H_i^{\cdot}] + 2[Vö] = [In'_{Sn}] = \text{constant} \quad (11)$$

Generally, oxygen vacancies are equilibrium with O_2 in the surrounding atmosphere, which can be expressed using Kröger–Vink notation[26]:

$$1/2O_2 + Vö + 2e^- \rightleftharpoons Oo^x \quad (12)$$

where Oo^x refers to a normal lattice oxide ion. Therefore, $Sn_{0.9}In_{0.1}P_2O_7$ shows an activity for O_2-exhange reaction that is similar to oxygen storage capacity. Probably, this is the reason for high propane conversions under rich conditions.

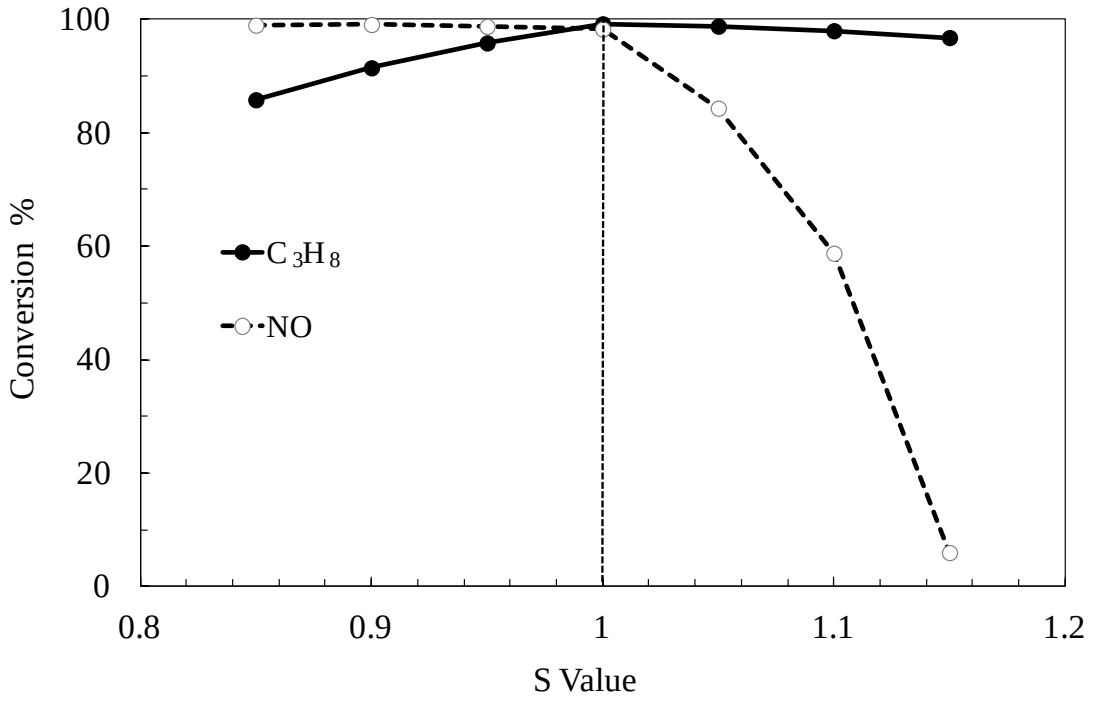

Figure 3-10 Influence of SV on propane and NO conversions at 450 °C. The propane, NO, O_2, and H_2O concentrations were kept constant at 1000 ppm, 1000 ppm, 4500 ppm, and 3 vol%, respectively.

The SV of the reactant gas is also of great important for practical applications. Figure

3-11 shows while the influence of the SV on propane conversion was relatively small, that on NO conversion was significant. The former result is similar to that for propane oxidation over the $Pt/Sn_{0.9}In_{0.1}P_2O_7$ catalyst, which reflects that the formation of active oxygen species is independent of the SV value. The latter result is mainly due to a decrease in the selectivity toward NO reduction at the cathodic site in the local electrochemical cell. As described earlier, this reaction competes with the oxygen reduction reaction shown in Eq. (9). It is likely that the adsorption of NO is suppressed at high SV values. However, the sensitivities toward NO would be improved by the addition of a basic material such as alkaline earth carbonates to the $Pt\text{-}Rh/Sn_{0.9}In_{0.1}P_2O_7$ catalyst, which provides additional adsorption sites for NO [27].

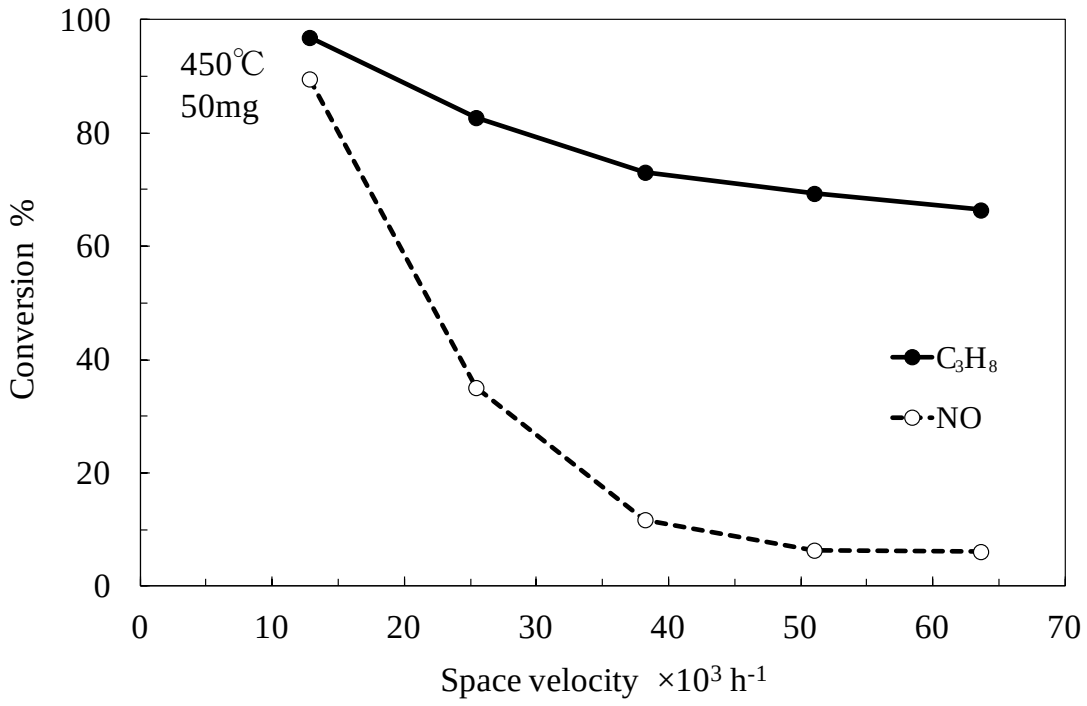

Figure 3-11 Influence of S value on propane and NO conversions at 450 °C. A constant SV of 9500 h^{-1} was maintained by controlling the amount of $\alpha\text{-}Al_2O_3$ additives.

3.4. Summary

The present study has proposed a concept for the propane and NO reaction at the proton conductor-electrocatalyst interface and has explored this reaction over untra-low Pt/ and Pt-Rh/$Sn_{0.9}In_{0.1}P_2O_7$ catalysts. In an electrochemical cell, propane was oxidized to CO_2 through the electrolysis of H_2O vapor at the anode. NO was reduced to N_2O through the reaction of proton with electron at the cathode. These electrochemical reactions also occurred at the same electrode in a half-cell when propane, H_2O, and NO were present in the reaction system. This phenomenon was further applicable to the Pt/$Sn_{0.9}In_{0.1}P_2O_7$ catalyst. Compared with a Pt/γ-Al_2O_3 catalyst, this catalyst showed significantly larger TOF values for Pt, thus providing higher catalytic activity at low temperatures and smaller quantities of Pt. The addition of Rh to Pt further enhanced the NO reduction activity by promoting the dissociative adsorption of NO at 300 ℃ or higher. With such activity, the Pt-Rh/$Sn_{0.9}In_{0.1}P_2O_7$ catalyst (0.01 wt% Pt, 0.005 wt% Rh) exhibited T50% of 285 and 355 ℃ for propane oxidation and NO reduction, respectively. Finally, the influence of the O_2 concentration in the reactant gas and its SV on the activity of Pt-Rh/$Sn_{0.9}In_{0.1}P_2O_7$ catalyst was also examined.

3.5 Reference

[1] H.S. Gandhi, G.W. Graham, and R.W. McCabe, Automotive exhaust catalysis, *J Catal*. **216**(1-2), 433-442 (2003).

[2] M.V. Twigg, Roles of catalytic oxidation in control of vehicle exhaust emissions, *Catal Today*. **117**(4), 407-418 (2006).

[3] S.I. Matsumoto, Recent advances in automobile exhaust catalysts, *Catal Today*. **90**(3-4), 183-190 (2004).

[4] R. Moller, C.H. Onder, L. Guzzella, M. Votsmeier, and J. Gieshoff, Analysis of a kinetic model describing the dynamic operation of a three-way catalyst, *Appl Catal B-Environ*. **70**(1-4), 269-275 (2007).

[5] Y. Yazawa, H. Yoshida, N. Takagi, S. Komai, A. Satsuma, and T. Hattori, Acid strength of support materials as a factor controlling oxidation state of palladium catalyst for propane combustion, *J Catal*. **187**(1), 15-23 (1999).

[6] B. Grbic, N. Radic, B. Markovic, P. Stefanov, D. Stoychev, and T. Marinova, Influence of manganese oxide on the activity of Pt/Al_2O_3 catalyst for CO and n-hexane oxidation, *Appl Catal B-Environ*. **64**(1-2), 51-56 (2006).

[7] H. Muraki, H. Shinjoh, H. Sobukawa, K. Yokota, and Y. Fujitani, Palladium Lanthanum Catalysts for Automotive Emission Control, *Ind Eng Chem Prod Rd*. **25**(2), 202-208 (1986).

[8] H. Muraki, K. Yokota, and Y. Fujitani, Nitric-Oxide Reduction Performance of Automotive Palladium Catalysts, *Appl Catal*. **48**(1), 93-105 (1989).

[9] H. Muraki, H. Shinjoh, and Y. Fujitani, Effect of Lanthanum on the No Reduction over Palladium Catalysts, *Appl Catal*. **22**(2), 325-335 (1986).

[10] Z. Hu, C.Z. Wan, Y.K. Lui, J. Dettling, and J.J. Steger, Design of a novel Pd three-way catalyst: Integration of catalytic functions in three dimensions, *Catal Today*. **30**(1-3), 83-89 (1996).

[11] A. Martinez-Arias, M. Fernandez-Garcia, A.B. Hungria, A. Iglesias-Juez, K. Duncan, R. Smith, J.A. Anderson, J.C. Conesa, and J. Soria, Effect of thermal sintering on light-off performance of $Pd/(Ce,Zr)_{O-x/}Al_2O_3$ three-way catalysts: Model gas and engine tests, *J Catal*. **204**(1), 238-248 (2001).

[12] G.F. Li, Q.Y. Wang, B. Zhao, and R.X. Zhou, The promotional effect of transition metals on the catalytic behavior of model $Pd/Ce_{(0.67)}Zr_{(0.33)}O_{(2)}$ three-way catalyst, *Catal Today*. **158**(3-4), 385-392 (2010).

[13] K.M. Adams and H.S. Gandhi, Palladium Tungsten Catalysts for Automotive Exhaust Treatment, *Ind Eng Chem Prod Rd*. **22**(2), 207-212 (1983).

[14] A. Papavasiliou, A. Tsetsekou, V. Matsouka, M. Konsolakis, and I.V. Yentekakis, An investigation of the role of Zr and La dopants into $Ce_{1-x-y}Zr_xLa_yO$ delta enriched gamma-Al2O3 TWC washcoats, *Appl Catal a-Gen*. **382**(1), 73-84 (2010).

[15] P. Heo, K. Ito, A. Tomita, and T. Hibino, A proton-conducting fuel cell operating with hydrocarbon fuels, *Angew Chem Int Edit*. **47**(41), 7841-7844 (2008).

[16] K. Tsuneyama, S. Tetanishi, T. Hibino, S. Nagao, H. Hirata, and S. Matsumoto, Low-temperature hydrocarbon combustion over proton conductor/metal-mixed catalysts, *J Catal*. **273**(1), 59-65 (2010).

[17] E. Shustorovich and A.T. Bell, Decomposition and Reduction of No on Transition-Metal Surfaces - Bond Order Conservation Morse Potential Analysis, *Surf Sci*. **289**(1-2), 127-138 (1993).

[18] M. Nagao, T. Yoshii, T. Hibino, M. Sano, and A. Tomita, Electrochemical reduction of NOx at intermediate temperatures using a proton-conducting In3+-doped SnP2O7 electrolyte, *Electrochem Solid St*. **9**(2), J1-J4 (2006).

[19] A. Tomita, T. Yoshii, S. Teranishi, M. Nagao, and T. Hibino, Selective catalytic reduction of NO_x by H^2 using proton conductors as catalyst supports, *J Catal*. **247**(2), 137-144 (2007).

[20] N. Miura, G.Y. Lu, N. Yamazoe, H. Kurosawa, and M. Hasei, Mixed potential type NOx sensor based on stabilized zirconia and oxide electrode, *J Electrochem Soc*. **143**(2), L33-L35 (1996).

[21] T. Hibino, A. Hashimoto, S. Kakimoto, and M. Sano, Zirconia-based potentiometric sensors using metal oxide electrodes for detection of hydrocarbons, *J Electrochem Soc*. **148**(1), H1-H5 (2001).

[22] X.G. Li and G.M. Kale, Influence of sensing electrode and electrolyte on performance of potentiometric mixed-potential gas sensors, *Sensor Actuat B-Chem*. **123**(1), 254-261 (2007).

[23] M. Machida, E. Shono, A. Kimura, and S. Yamauchi, Electrochemical lean-deNO(x) catalyst using H+-conducting solid polymer electrolyte, *Catal Commun*. **4**(12), 631-635 (2003).

[24] K.C. Taylor and J.C. Schlatter, Selective Reduction of Nitric-Oxide over Noble-Metals, *J Catal*. **63**(1), 53-71 (1980).

[25] X.L. Chen, C.S. Wang, E.A. Payzant, C.R. Xia, and D. Chu, An Oxide Ion and Proton Co-Ion Conducting $Sn_{0.9}In_{0.1}P_2O_7$ Electrolyte for

Intermediate-Temperature Fuel Cells, *J Electrochem Soc*. **155**(12), B1264-B1269 (2008).

[26] F.A. Kroger and H.J. Vink, Relations between the Concentrations of Imperfections in Crystalline Solids, *Solid State Phys*. **3** 307-435 (1956).

[27] M. Misono and T. Inui, New catalytic technologies in Japan, *Catal Today*. **51**(3-4), 369-375 (1999).

CHAPTER IV

Mechanism Discussion over Proton Conductor Supported PtRh Three Way Catalysts

4.1. Introduction

So far, the catalytic purification of emissions from gasoline engines has been commonly performed by three-way catalyst (TWC), which is mainly supported Pt-Rh-Pd catalysts [1-3]. In the three-way catalysis, unburned hydrocarbons (HCs) and carbon monoxide (CO) are oxidized, and at the same time, produced nitrogen oxides (NO_x) are reduced, which is accomplished by controlling the air/fuel ratio of the exhaust close to a stoichiometric value of 14.6. The addition of ceria or the related compounds to TWCs promotes both the HC oxidation under fuel-rich conditions and the NO_x reduction under fuel-lean conditions [4-6]. γ-alumina with high surface area and good thermal tolerance is widely employed as the catalyst support for TWCs[7].

As a heterogeneous catalyst, the reaction scheme over the TWCs is very complicated. Generally, reactions on the noble metal surface are explained using Langmuir–Hinshelwood kinetics and reactions on the ceria surface mainly follow the Eley–Rideal mechanism[8]. However, in most cases, the electrochemical mechanism is not involved, which is mainly adopted and discussed in the electrochemical sensors. The catalyst support is an important component in TWCs for enhancing the dispersion of

reaction sites; however, it has a remarkably smaller effect on the reaction scheme. But as we have proposed a new scheme for propane+NO+oxygen reaction over the TWC using $Sn_{0.9}In_{0.1}P_2O_7$ (SIPO) as a catalyst support. SIPO is a pure proton conductor, showing high proton conductivities above 0.05 S cm^{-1} in the temperature range of 100–400 °C. This compound is also thermally resistant until at least 1000 °C. In the presence of water vapor, this molecule is dissociated into protons and electrons at anodic sites at the proton conductor–catalyst interface and the resultant active oxygen oxidizes propane to CO_2 via Eq. (1). Separately, NO reacts with protons and electrons to form N_2 at cathodic sites at the proton conductor–catalyst interface via Eq. (2).

$$C_3H_8 + 6H_2O \rightarrow 3CO_2 + 20H^+ + 20e^- \quad (1)$$

$$10NO + 20H^+ + 20e^- \rightarrow 5N_2 + 10H_2O \quad (2)$$

Under stoichiometric conditions, including 1000 ppm propane, 1000 ppm NO, 4500 ppm O_2, and 3 % water vapor, the temperatures at which the above series of reactions could achieve 50% conversion ($T_{50\%}$) were 330 and 360 °C for propane and NO, respectively, over a 0.01 wt% Pt-0.005 wt% Rh/SIPO catalyst. This performance is superior to that of a 1 wt% Pt/γ-alumina catalyst, which is used as a standard catalyst at Toyota Motor Corporation, under the same conditions.

The objective of the study in this chapter is to validate the reaction scheme represented in Eqs. (1) and (2) by relating the catalytic activity for the propane and NO reaction to proton conduction in the catalyst supports. Besides SIPO, three proton conductors of $Sn_{0.95}Al_{0.05}P_2O_7$ (SAPO), $Sn_{0.9}Mg_{0.1}P_2O_7$ (SMPO), and $Fe_{0.5}Nb_{0.5}P_2O_7$ (FNPO) were used as catalyst supports for Pt and Rh. These proton conductors have a cubic structure similar to that of ZrP_2O_7, but show different proton conductivities at intermediate temperatures [9]. Here, we report a large dependency of the activity of the

four catalysts for the propane oxidation and NO reduction reactions on the support species. The four catalysts were characterized using BET surface area, x-ray diffraction (XRD), transmission electron microscopy (TEM), and proton magic angle spinning (MAS) nuclear magnetic resonance (NMR) measurements. The propane oxidation and NO reduction reactions over the four catalysts were further inspected from electrochemical techniques, including current–voltage curve and electrode potential measurements. Finally, the dependency of the catalytic activity on the catalyst support species was discussed in terms of the proton concentration and mobility in the bulk of the catalyst supports.

4.2. Experimental Section

4.2.1. Materials

Catalyst supports of SIPO, SAPO, and SMPO were prepared according to the procedure reported previously [10-13] . SnO_2 (C. I. Kasei) and In_2O_3, $Al(OH)_3$, or MgO (Wako) were mixed with 85% H_3PO_4 and de-ionized water, and stirred at 300 °C until a high viscosity paste was formed. The paste was calcined in an alumina pot at 650 °C for 2.5 h and then ground in a mortar. FNPO was synthesized from Fe_2O_3 and Nb_2O_5 (Wako) in a similar manner to that described above, although the paste was calcined at 450 °C [13]. For catalyst studies, SIPO-, SAPO-, SMPO-, and FNPO-supported Pt-Rh catalysts (0.01 wt% Pt content and 0.005 wt% Rh content) were prepared by impregnation of the support powder surface with Pt and Rh precursors. The support powder was suspended in de-ionized water, and two aqueous solutions of

$Pt(NH_3)_4Cl_2 \cdot H_2O$ and $(NH_4)_3RhCl_6 \cdot H_2O$ were added dropwise to the suspension using micropipettes while stirring at approximately 60 °C. After aging at this temperature overnight, the catalyst powder was oxidized in an air feed at 300 °C for 1 h and then reduced in a 10 vol% H_2 (argon balance) feed at 450 °C for 1 h. For electrochemical cell studies, the SIPO, SAPO, SMPO, and FNPO powders were uniaxially pressed into pellets (12 mm diameter, ca. 1 mm thick) under a pressure of 100 MPa for use as the electrolyte. A Pt-Rh/C (10 wt% Pt-Rh/C, Pt:Rh = 2:1) electrode with a gas diffusion layer was purchased from BASF.

4.2.2. Characterization

The BET surface area of SIPO, SAPO, SMPO, and FNPO was measured using a Micromeritics automated particle analyzer system. The sample was degassed under vacuum at 100 °C for 1 h and then at 250 °C for 3 h prior to BET measurements. The BET measurements were carried out using krypton as an absorbent at –195 °C. The structural parameters of SIPO, SAPO, SMPO, and FNPO were analyzed using X-ray diffraction (XRD). XRD patterns were collected using a Rigaku Miniflex II diffractometer with Cu Kα radiation (λ=1.5432 Å) as the X-ray source. The diffractometer was operated at 45 kV and 20 mA. The environment of protons in the bulk of SIPO, SAPO, SMPO, and FNPO was monitored using ^1H MAS NMR measurements. The NMR experiments were performed using a Chemagnetics CMX-300 NMR spectrometer at room temperature in a feed of dry N_2. The chemical shift and the relaxation time, T_1, were recorded at a 90° pulse length of 4 μs and a decay time between pulses of 5 s. The spinning rate of the sample was set to 9 kHz. The dispersion state of PtRh alloys in the catalyst was characterized using transmission electron microscopy (TEM: JEOL JEM2100F) in conjunction with energy dispersive X-ray

(EDX: JEOL JED-2300T) spectroscopy. Specimens for the TEM measurements were prepared by ultrasonic dispersion in *n*-butanol, and a drop of the resultant suspension was evaporated on a Cu grid.

4.2.3. Catalyst studies

The activity of the catalysts obtained above for the HC oxidation and NO reduction reactions was measured under various conditions. Catalytic tests were conducted in a fixed-bed flow reactor with 100 mg of catalyst that was mixed with 100 mg of α-alumina in a mortar for a few minutes. A mixture of 1000 ppm propane, 1000 ppm NO, 4500 ppm O_2, and 3 % water vapor in Ar was fed into the reactor, wherein the space velocity (SV) was in the range of 300 to 9500 h^{-1}. The concentrations of propane and NO_x in the outlet gas were monitored using an on-line Varian CP-2002 chromatograph and Horiba PG-225 NO_x gas analyzer, respectively. The gas concentrations were obtained after the reaction had achieved a steady state.

4.2.4. Electrochemical cell studies

The HC oxidation and NO reduction reactions shown in Eqs. (1) and (2), respectively, were investigated using an electrochemical cell. The two Pt-Rh/C electrodes (area: 0.5 cm^2) were attached to opposite sides of the electrolyte. Two electrode chambers were set up by placing the cell assembly between two alumina tubes. A mixture of 1000 ppm propane and 3% water vapor in argon was supplied to the Pt-Rh/C anode at a flow rate of 30 mL min^{-1}, and 1000 ppm NO diluted with argon was supplied to the Pt-Rh/C cathode at a flow rate of 30 mL min^{-1}. The current–voltage curves were measured using a Hokuto Denko HA-501 galvanostat at 200 °C. The potentials of the anode and cathode were separated by attaching a Pt reference electrode to the side of the electrolyte.

4.3. Results and Discussion

4.3.1. Propane oxidation and NO reduction reactions over the proton conductors-supported Pt-Rh catalysts

The activity of the Pt-Rh/proton conductor catalysts for the propane oxidation and NO reduction reactions was measured using a mixture feed of propane, NO, O_2, and water vapor in argon. The propane and NO conversions as a function of the temperature are shown in Figure 4-1. The results showed that the activity of those catalysts were significantly dependent on the used catalyst support species. The ignition temperatures for propane oxidation and NO reduction were 250 and 250 ℃, respectively, over Pt-Rh/FNPO, 250 and 300 ℃, respectively, over Pt-Rh/SIPO, 300 and 350 ℃, respectively, over Pt-Rh/SAPO, and 350 and 400 ℃, respectively, over Pt-Rh/SMPO. Even larger differences were observed for $T_{50\%}$: $T_{50\%}$ for propane oxidation was 313, 330, 405, and 550 ℃ for Pt-Rh/FNPO, Pt-Rh/SIPO, Pt-Rh/SAPO, and Pt-Rh/SMPO, respectively; $T_{50\%}$ for NO reduction was 330, 360, 465, and over 600 ℃ for Pt-Rh/FNPO, Pt-Rh/SIPO, Pt-Rh/SAPO, and Pt-Rh/SMPO, respectively.

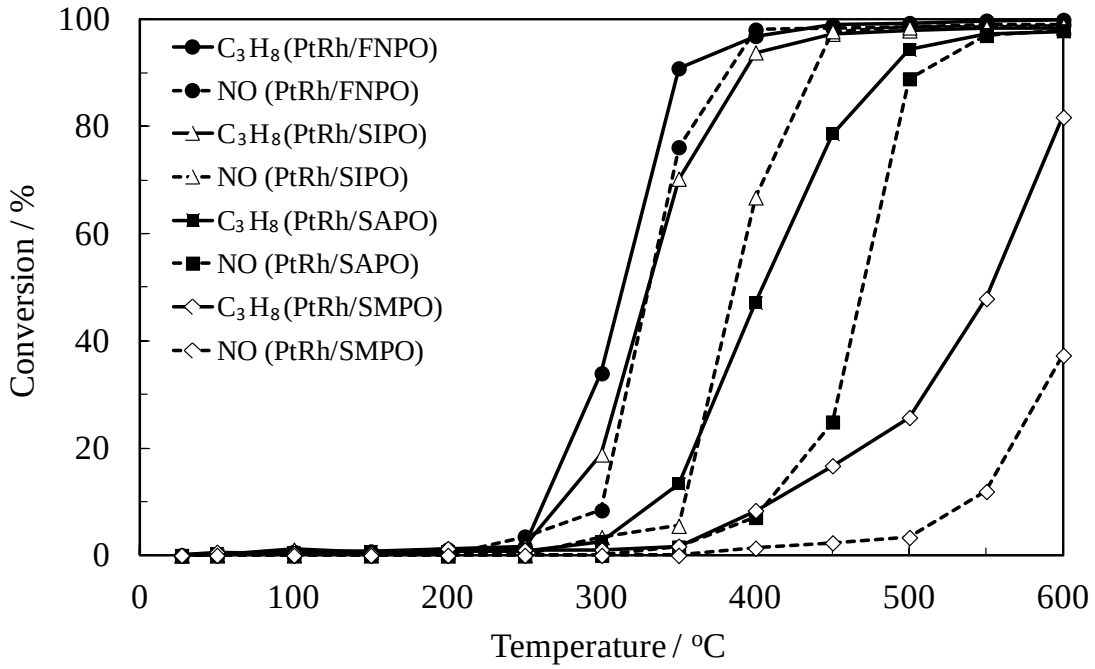

Figure 4-1 Propane and NO conversions as a function of temperature for Pt-Rh/SnP_2O_7-based proton conductor catalysts. The reactant gas was 1000 ppm propane, 1000 ppm NO, 4500 ppm O2, and 3 % water vapor in Ar.

The influence of the SV on the propane oxidation and NO reduction reactions over the Pt-Rh/proton conductor catalysts was investigated at 450 °C. Figure 4-2 shows the propane and NO conversions as a function of the SV. The results were also influenced by the used catalyst support species. Both the propane and NO conversions over Pt-Rh/FNPO and Pt-Rh/SIPO were kept constant at approximately 95% in the tested SV range, where the propane and NO conversions over Pt-Rh/FNPO were slightly higher than those over Pt-Rh/SIPO. In contrast, the propane and especially NO conversions over Pt-Rh/SAPO were decreased by the increase in SV. More significantly, both the propane and NO conversions over Pt-Rh/SMPO were always 10% or less at all the tested SV values.

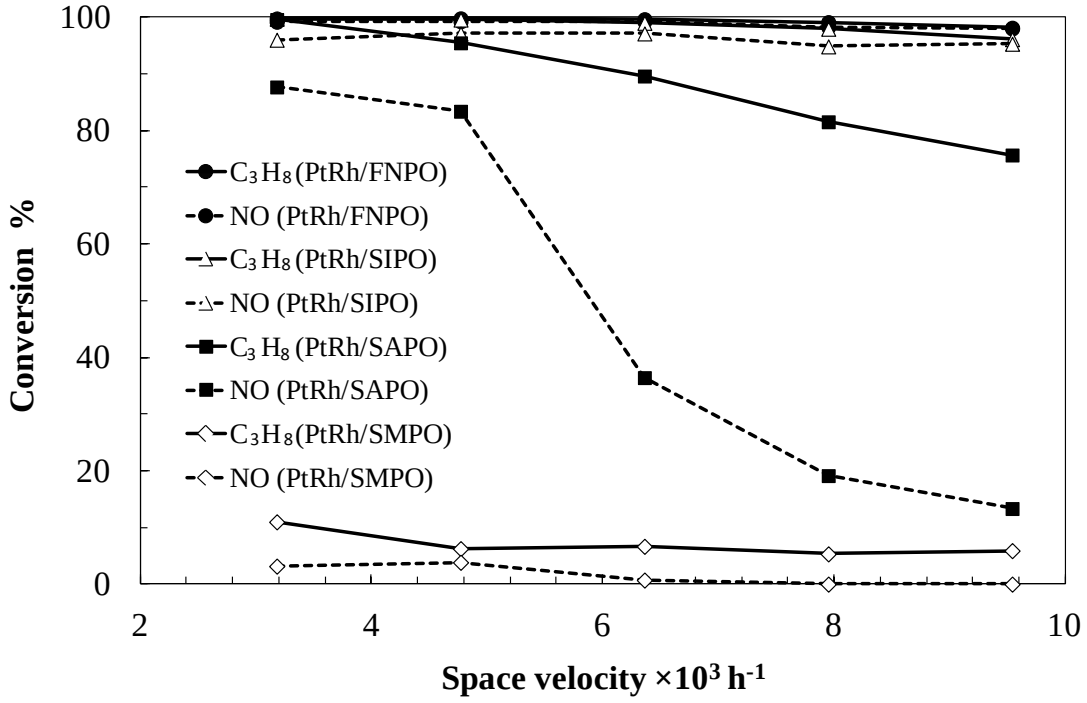

Figure 4-2 Propane and NO conversions as a function of the SV for Pt-Rh/SnP_2O_7-based proton conductor catalysts. The reactant gas was 1000 ppm propane, 1000 ppm NO, 4500 ppm O_2, and 3 % water vapor in Ar.

Based on the above observations, it is concluded that the difference in activity of the four catalysts for propane oxidation and NO reduction is significant. To clarify whether this difference is simply attributable to the difference in surface area of the catalyst supports or dispersion of PtRh particles on its surface, the BET, XRD, and TEM measurements were performed.

Table 4-1 summarizes the BET surface areas measured by the krypton absorption and particle sizes estimated from of the four catalyst supports XRD spectra by using the Scherrer formula. The BET surface areas of the used catalyst supports were between 2.6 and 8.8 $m^2\ g^{-1}$ and their particle sizes were approximately 40-50 nm, where there is no correlation of the catalytic activity with these factors. Also, only very slight differences

were found in the XRD spectra, which confirmed that the four materials shared similar proton conductive structure.

Figure 4-3 shows the TEM images of the four catalysts. The particle sizes of PtRh were 7 nm or smaller for all the catalysts and their dispersion state was seen to be similar among the catalysts. In addition, the EDX spectra of the PtRh particle on the surface of the four catalysts showed that the composition was in agreement with that of the preparative source materials within experimental error (data not shown). We thus can neglect the physical factors such as the surface area and the PtRh dispersion state in considering the difference in activity among the catalysts.

Table 4-1 BET surface areas and particle sizes of SnP_2O_7-based proton conductors.

	BET surface area/ m^2 g^{-1}	**Particle size/ nm**
$Fe_{0.5}Nb_{0.5}P_2O_7$	2.6	53
$Sn_{0.9}In_{0.1}P_2O_7$	7.4	42
$Sn_{0.95}Al_{0.05}P_2O_7$	8.4	43
$Sn_{0.9}Mg_{0.1}P_2O_7$	5.6	45

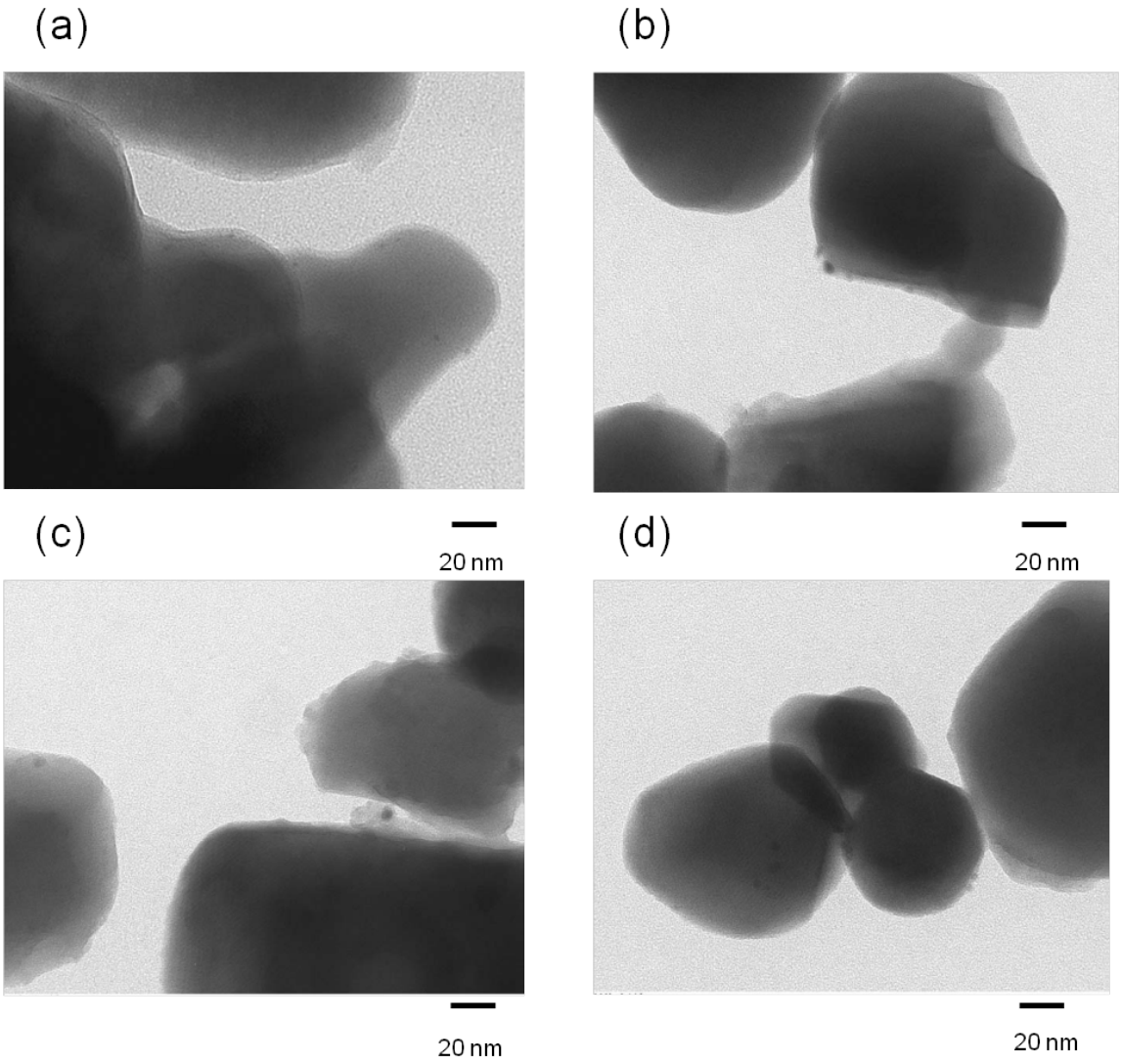

Figure 4-3 TEM images of SnP_2O_7-based proton conductor catalysts. The Pt and Rh contents were 0.01 and 0.005 wt%, respectively.

4.3.2. Propane oxidation and NO reduction reactions at the Pt-Rh/C electrode in an electrochemical cell

The propane oxidation and NO reduction reactions shown in Eqs. (1) and (2), respectively, were inspected using the Pt-Rh/C electrode attached on the surface of the FNPO, SIPO, SAPO, and SMPO electrolytes. Based on the mixed potential mechanism

[14-17], propane is oxidized to CO_2 through Eq. (1) at anodic sites on the Pt-Rh/C electrode, giving rise to a negative potential due to rich electrons. On the other hand, NO is reduced to N_2 through Eq. (2) at cathodic sites on the same Pt-Rh/C electrode, giving rise to a positive potential due to poor electrons. (The appearance of the anode and cathode sites on the PtRh particle is thought to be due to the heterogeneity of the metal surface, which results from the difference in the atomic lattice and structure defects.) As a result, a local galvanic cell is formed at the same Pt-Rh/C electrode in a mixture of propane, NO, and water vapor. Since the electrode also functions as a lead wire, the cell becomes short-circuited. In this case, the rates of the reactions shown in Eqs. (1) and (2) are equal, resulting in the progress of the following overall reaction.

$$C_3H_8 + 10NO \rightarrow 3CO_2 + 4H_2O + 5N_2 \qquad (3)$$

Therefore, the rate of the reaction shown in Eq. (3) corresponds to the short-circuit current value of the local galvanic cell; however, this short-circuit current value cannot actually be measured due to the occurrence at the same electrode. We thus estimated the short-circuit current from the current–voltage curve of the electrochemical cell, wherein a mixture of propane and H_2O in argon was supplied to the anode and NO diluted with argon was supplied to the cathode. Figure 4-4 displays that the short-circuit current values were 0.7, 0.45, 0.35, and 0.12 mA for the FNPO, SIPO, SAPO, and SMPO electrolytes, respectively. This order is the same as that of the activity of the Pt-Rh/proton conductor catalysts shown in Figures 4-1 and 4-2, which suggests that propane oxidation and NO reduction over the Pt-Rh/proton conductor catalysts proceed according to Eqs. (1) and (2), respectively. Interestingly, the difference in short-circuit current observed in Figure 3 is not only owing to that in the internal resistance of the cells, but also owing to that in their open-circuit voltage. Before discussing these points

later, the potentials of the anode and cathode against the reference electrode were measured under open-circuit conditions, and the results are summarized in Table 4-2. While the anode potential became more negative in the order of FNPO > SIPO > SAPO > SMPO, the cathode potential became less negative in the same order as shown above. Moreover, the difference in cathode potential among the cells is somewhat larger than that in anode potential among the cells. It is likely that the cathode potential is more significantly determined by the kinetics of NO reduction rather than its equilibrium when compared to the anode potential.

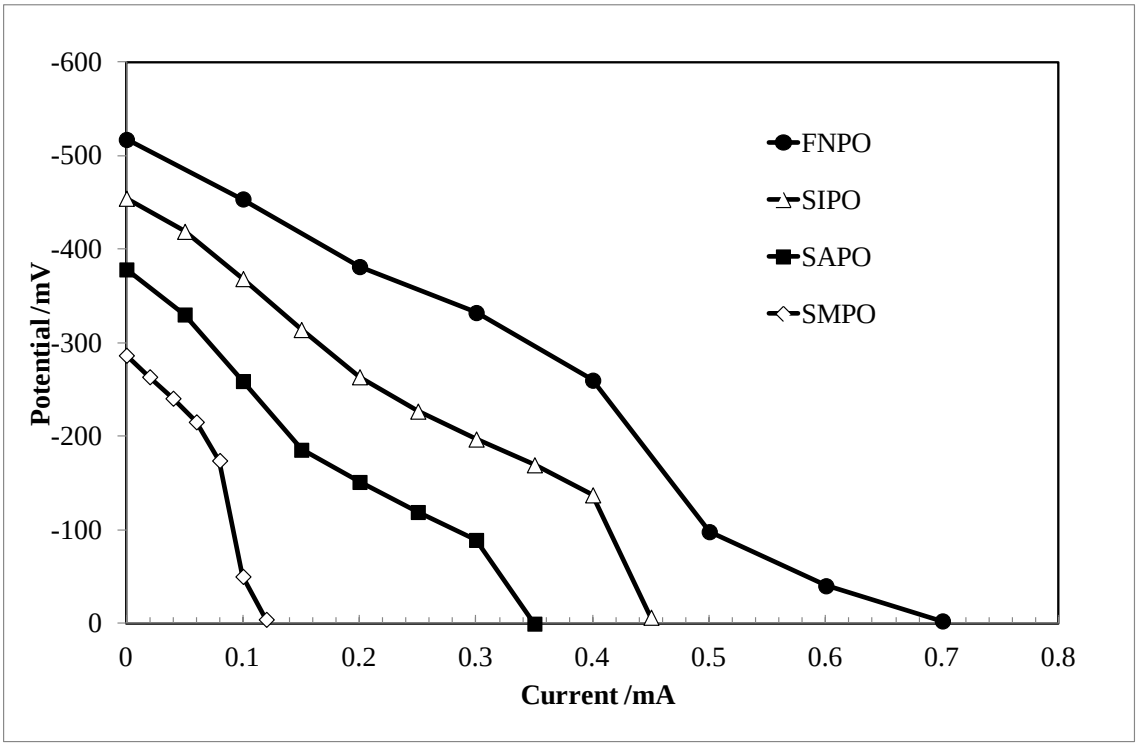

Figure 4-4 Current–voltage curve of the four electrochemical cells with FNPO, SIPO, SAPO, and SMPO as electrolytes at 200 °C. The short-circuit currents were estimated at a potential of 0 mV. A mixture of 1000 ppm propane and 3 vol% H_2O in Ar was supplied to the anode, and 1000 ppm NO diluted with Ar was supplied to the cathode.

Table 4-2 Potentials of the anode and cathode against the reference electrode under open-circuit conditions at 200 °C.

	Propane oxidation/mV	**NO reduction/mv**
$Fe_{0.5}Nb_{0.5}P_2O_7$	-643	-126
$Sn_{0.9}In_{0.1}P_2O_7$	-603	-149
$Sn_{0.95}Al_{0.05}P_2O_7$	-570	-190
$Sn_{0.9}Mg_{0.1}P_2O_7$	-556	-267

A mixture of 1000 ppm propane and 3 vol% H_2O in Ar was supplied to the anode, and 1000 ppm NO diluted with Ar was supplied to the cathode.

4.3.3. Proton conduction in the four proton conductors

Figure 4-5 shows the dependence of the proton conductivities of FNPO, SIPO, SAPO, and SMPO on the temperature, in addition to the activation energy values estimated from the slopes obtained in the linear region of the Arrhenius plots. The order of the proton conductivity was FNPO > SIPO > SAPO > SMPO, while the activation energy of SMPO (28 kJ mol^{-1}) was higher than those of the other three samples (*ca.* 21kJ mol^{-1}), the behaviors of which well correspond to the catalytic activity of Pt-Rh supported on the surface of these proton conductors. Considering the similarity in the structural features among the four proton conductors (Table 4-1), the observed difference in proton conduction is related to the concentration and mobility of protons in the bulk of the samples. A comparison between these factors for the samples was made to clarify this point as below.

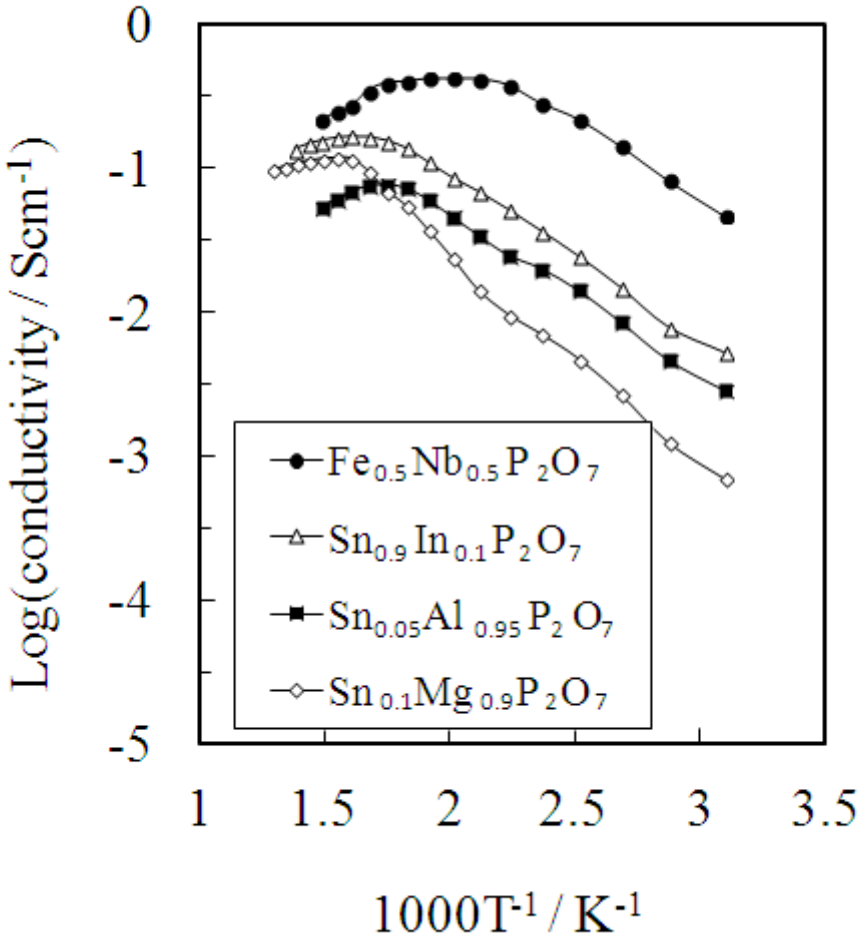

Figure 4-5 Dependence of the proton conductivities of SnP_2O_7-based proton conductors on the temperature

^{1}H MAS NMR spectra of FNPO, SIPO, SAPO, and SMPO are shown in Figure 4-6. Although a large peak was observed for each sample, it appeared the different chemical shift values. In particular, the chemical shift of protons in SMPO was extremely small. It is worth noting that the chemical shift of protons is closely related to the strength of the hydrogen bond (-O−H···O-); the peak shifts to a higher magnetic field corresponding to a longer hydrogen bonding distance [18, 19]. This suggests that the

protons are the most strictly restricted to the lattice oxide ions in SMPO. Evidence for this is provided by the relaxation time, T_1, for the three samples. (The T_1 value for FNPO cannot be measured due to its paramagnetism.) Table 4-3 shows that the T_1 value increased in the order of SAPO ≤ SIPO << SMPO, which reflects the proton mobility being restricted in this order[20]. Proton mobility is thought to be affected by the charge density of the dopants in SnP_2O_7, since they have negative charges, inhibiting proton transport as reported for doped $La_2Zr_2O_7$ [21]. It is possible that this effect is more prominent when doping with divalent Mg^{2+} than when doping with trivalent In^{3+} and Al^{3+}, thus causing the lower proton conductivity and the higher activation energy (Table 4-3).

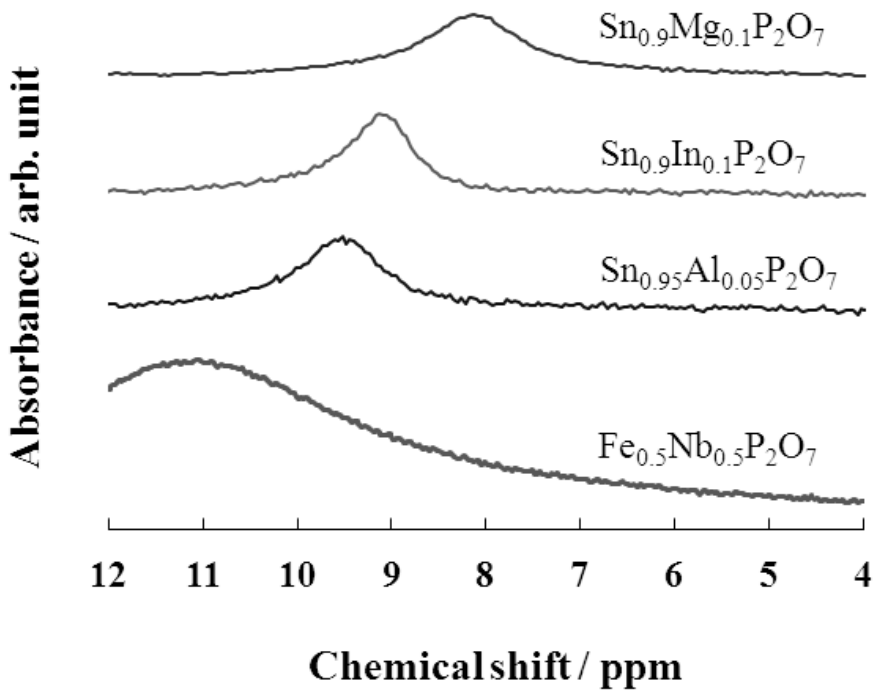

Figure 4-6 ^{1}H MAS NMR spectra of SnP_2O_7-based proton conductors.

Table 4-3 The relaxation time, T_1, of SnP_2O_7-based proton conductors.

	Relaxation Time/s
$Fe_{0.5}Nb_{0.5}P_2O_7$	/
$Sn_{0.95}Al_{0.05}P_2O_7$	0.03 sec
$Sn_{0.9}In_{0.1}P_2O_7$	0.04 sec
$Sn_{0.9}Mg_{0.1}P_2O_7$	0.10 sec

4.3.4. A relationship between catalytic activity and proton conduction

As described earlier, the short-circuit current of the electrochemical cell is determined by both its internal resistance and cathode potential. Of these factors, the internal resistance can correlate with the proton conductivity of the electrolyte. In our reaction scheme, protons migrate from the anodic site to the cathodic site through the proton conductor. Accordingly, a higher proton conductivity causes a larger short-circuit current, which is reflected by the difference in slope of the current–voltage curve among the cells (Fig. 4-4). In contrast, it is difficult to relate the cathode potential directly to the proton conductivity (Table 4-2). A possible explanation is that the rate of NO reduction shown in Eq. (2) is slow, so that the electrode becomes less positive, especially in the cell with the SMPO electrolyte[22]. For NO reduction, protons must be extracted from the bulk of the proton conductor. In this case, the protons are subject to the largest restriction from the lattice oxide ions in SMPO (Fig. 4-6), which may result in a remarkably low rate of NO reduction at the electrode.

Based on the above observations and discussions, the effect of the support species on the activity of the Pt-Rh/proton conductor catalysts can be accounted for by proton

conduction in the used supports, which strongly suggests that the reaction shown in Eq. (3) over the Pt-Rh/proton conductor catalysts proceeds according to the mixed potential mechanism. The above effect might also be explained by the acidity of the catalyst supports. However, note that the NH_3–desorption profiles for SIPO and SAPO were very similar in temperature-programmed desorption (TPD) measurements.

4.4. Summary

The relationship between the activity of the proton conductors-supported Pt-Rh catalysts for propane+NO+O_2 reaction and proton conduction in the used catalyst supports was investigated to demonstrate the reaction scheme based on the mixed potential mechanism. FNPO, SIPO, SAPO, and SMPO, which have a similar BET surface area and particle size but show different proton conductivities, were used as catalyst supports. The activity of these catalysts was significantly dependent on the catalyst support species. $T_{50\%}$ for propane oxidation was 313, 330, 405, and 550 °C for Pt-Rh/FNPO, Pt-Rh/SIPO, Pt-Rh/SAPO, and Pt-Rh/SMPO, respectively. $T_{50\%}$ for NO reduction was 330, 386, 465, and over 600 °C for Pt-Rh/FNPO, Pt-Rh/SIPO, Pt-Rh/SAPO, and Pt-Rh/SMPO, respectively. Furthermore, Pt-Rh/FNPO and Pt-Rh/SIPO maintained high propane and NO conversions in the tested SV range, whereas Pt-Rh/SMPO showed propane and NO conversions of 10% or less at all the tested SV values. This dependence on the catalyst support species could be successfully explained by incorporating the difference in proton conduction among the catalyst supports into the mixed potential mechanism. According to this new mechanism, since protons migrate from the anodic site to the cathodic site through the proton conductor, a higher proton conductivity results in a larger short-circuit current of the local galvanic

cell. In addition, since the anodic and especially cathodic potentials are determined by the rate of the proton exchange reaction between the reactant gas and the lattice oxide ion, the faster proton mobility causes the higher open-circuit voltage of the local galvanic cell. Finally, we emphasize that the use, especially of FNPO, as the catalyst support could reduce significantly the Pt and Rh content while maintaining high catalytic activity.

4.5 References

[1] M.V. Twigg, Roles of catalytic oxidation in control of vehicle exhaust emissions, *Catal Today*. **117**(4), 407-418 (2006).

[2] S.I. Matsumoto, Recent advances in automobile exhaust catalysts, *Catal Today*. **90**(3-4), 183-190 (2004).

[3] R.M. Heck and R.J. Farrauto, Automobile exhaust catalysts, *Appl Catal a-Gen*. **221**(1-2), 443-457 (2001).

[4] T. Bunluesin, R.J. Gorte, and G.W. Graham, Studies of the water-gas-shift reaction on ceria-supported Pt, Pd, and Rh: implications for oxygen-storage properties, *Appl Catal B-Environ*. **15**(1-2), 107-114 (1998).

[5] E.V. Kondratenko, Y. Sakamoto, K. Okumura, and H. Shinjoh, Transient analysis of oxygen storage capacity of Pt/CeO_2-ZrO_2 materials with millisecond- and second-time resolution, *Appl Catal B-Environ*. **89**(3-4), 476-483 (2009).

[6] N.R. Collins and M.V. Twigg, Three-way catalyst emissions control technologies for spark-ignition engines - recent trends and future developments, *Top Catal*. **42-43**(1-4), 323-332 (2007).

[7] M.V. Twigg, Catalytic control of emissions from cars, *Catal Today*. **163**(1), 33-41 (2011).

[8] R. Moller, C.H. Onder, L. Guzzella, M. Votsmeier, and J. Gieshoff, Analysis of a kinetic model describing the dynamic operation of a three-way catalyst, *Appl Catal B-Environ*. **70**(1-4), 269-275 (2007).

[9] X. Dong, K. Tsuneyama, and T. Hibino, Ultra-low loading Pt Rh/Sn0.9In0.1P2O7 three-way catalyst for propane + NO + O_2 reaction, *Appl Catal B-Environ*.

106(3-4), 503-509 (2011).

[10] M. Nagao, T. Yoshii, T. Hibino, M. Sano, and A. Tomita, Electrochemical reduction of NOx at intermediate temperatures using a proton-conducting In3+-doped SnP2O7 electrolyte, *Electrochem Solid St*. **9**(2), J1-J4 (2006).

[11] A. Tomita, T. Yoshii, S. Teranishi, M. Nagao, and T. Hibino, Selective catalytic reduction of NO_x by H^2 using proton conductors as catalyst supports, *J Catal*. **247**(2), 137-144 (2007).

[12] K. Genzaki, P. Heo, M. Sano, and T. Hibino, Proton Conductivity and Solid Acidity of Mg-, In-, and Al-Doped SnP_2O_7, *J Electrochem Soc*. **156**(7), B806-B810 (2009).

[13] Y.B. Shen, K. Kojima, M. Nishida, P. Heo, K.H. Choi, H. Chang, and T. Hibino, Proton conduction in $A_{(0.5)}(III)B_{(0.5)}(V)P_{(2)}O_{(7)}$ compounds at intermediate temperatures, *J Mater Chem*. **22**(30), 14907-14915 (2012).

[14] N. Miura, G.Y. Lu, N. Yamazoe, H. Kurosawa, and M. Hasei, Mixed potential type NOx sensor based on stabilized zirconia and oxide electrode, *J Electrochem Soc*. **143**(2), L33-L35 (1996).

[15] R. Mukundan, E.L. Brosha, and F.H. Garzon, Mixed potential hydrocarbon sensors based on a YSZ electrolyte and oxide electrodes, *J Electrochem Soc*. **150**(12), H279-H284 (2003).

[16] X.G. Li and G.M. Kale, Influence of sensing electrode and electrolyte on performance of potentiometric mixed-potential gas sensors, *Sensor Actuat B-Chem*. **123**(1), 254-261 (2007).

[17] V.V. Plashnitsa, V. Gupta, and N. Miura, Mechanochemical approach for fabrication of a nano-structured NiO-sensing electrode used in a zirconia-based NO_2 sensor, *Electrochim Acta*. **55**(23), 6941-6945 (2010).

[18] H. Eckert, J.P. Yesinowski, L.A. Silver, and E.M. Stolper, Water in Silicate-Glasses - Quantitation and Structural Studies by H-1 Solid Echo and Mas-Nmr Methods, *J Phys Chem-Us*. **92**(7), 2055-2064 (1988).

[19] A. Matsuda, V.H. Nguyen, Y. Daiko, H. Muto, and M. Sakai, Three-dimensional hydrogen-bonding networks and proton conductivities under non-humidified conditions of CsHSO4-WPA composites, *Solid State Ionics*. **181**(3-4), 180-182 (2010).

[20] R. Brindle, M. Pursch, and K. Albert, H-1 MAS NMR spectroscopy of chemically modified silica gels: A fast method to characterize stationary interphases for chromatography, *Solid State Nucl Mag*. **6**(3), 251-266 (1996).

[21] M.E. Bjorketun, C.S. Knee, B.J. Nyman, and G. Wahnstrom, Protonic defects in

pure and doped $La_2Zr_2O_7$ pyrochlore oxide, *Solid State Ionics*. **178**(31-32), 1642-1647 (2008).

[22] H. Uchida, M. Yoshida, and M. Watanabe, Effects of Ionic Conductivities of Zirconia Electrolytes on Polarization Properties of Platinum Anodes in Solid Oxide Fuel-Cells, *J Phys Chem-Us*. **99**(10), 3282-3287 (1995).

CHAPTER V

General Conclusions

Two-way and three-way catalysts have been widely used to control the vehicle emissions, while reducing costs and improving cold start efficiency still remain big challenges of the catalysts. In this thesis, based on the novel proton conductive material $Sn_{0.9}In_{0.1}P_2O_7$, ultra low loading $Pt/Sn_{0.9}In_{0.1}P_2O_7$ and $PtRh/Sn_{0.9}In_{0.1}P_2O_7$ electrochemical catalysts were developed and tested in the two way and three way reactions, involving an innovative mixed potential mechanism.

The oxidation of propane and reduction of O_2 or N_2 were firstly tested in an electrochemical cell and then a half cell, where $Sn_{0.9}In_{0.1}P_2O_7$ and Pt/C was used as electrolyte and electrode separately; the high mixed potential and other cell performance results showed the reactions are spontaneous and high current efficiency in the electrochemical reactors. To increase the number of such active reactors which is formed on the interfacial with Pt and $Sn_{0.9}In_{0.1}P_2O_7$, the $Pt/Sn_{0.9}In_{0.1}P_2O_7$ and $PtRh/Sn_{0.9}In_{0.1}P_2O_7$ electrochemical catalysts were prepared. The $Sn_{0.9}In_{0.1}P_2O_7$ based catalysts exhibited the following important characteristics: high catalytic activities for hydrocarbons and NO, relatively low reaction temperature, and ultra low loading contents of Pt and Rh. For the two way process, the propane conversion reached approximately 90% at 400 °C even for 0.01 wt% Pt; for the three way process, the $Pt\text{-}Rh/Sn_{0.9}In_{0.1}P_2O_7$ catalyst (0.01 wt% Pt, 0.005 wt% Rh) exhibited T50% of 285 and 355 °C for propane oxidation and NO reduction, respectively. The results are much

better than the normal Pt/γ-Al_2O_3 and PtRh/γ-Al_2O_3 catalyst with the same or much higher loading amount.

In these electrochemical catalysts, the reactions are believed to occur on the interface between precious metals and the proton conductors. The relationship between the activity of the proton conductors-supported Pt-Rh catalysts for propane+NO+O_2 reaction and proton conduction in the used catalyst supports was carefully investigated to demonstrate the reaction scheme based on the mixed potential mechanism. FNPO, SIPO, SAPO, and SMPO, which have a similar BET surface area and particle size but show different proton conductivities, were used as catalyst supports. The activity and SV range of these catalysts was significantly dependent on the catalyst support species. This dependence on the catalyst support species could be successfully explained by incorporating the difference in proton conduction among the catalyst supports into the mixed potential mechanism. According to this new mechanism, since protons migrate from the anodic site to the cathodic site through the proton conductor, a higher proton conductivity results in a larger short-circuit current of the local galvanic cell. In addition, since the anodic and especially cathodic potentials are determined by the rate of the proton exchange reaction between the reactant gas and the lattice oxide ion, the faster proton mobility causes the higher open-circuit voltage of the local galvanic cell.

With the development of the proton conductive support materials and the further elucidation of the mechanism, new electrochemical catalysts will be developed to meet the advancing requirements.

Academic Publications

1. "Proton-Conductor-Supported Ultra-Low Loading Pt-Rh Three-way Catalysts", **Xue Dong**, Masakazu, and Takashi Hibino*, *Journal of Physical Chemistry C*, 2013, 117 (4), 1827–1832
2. "Ultra-low loading Pt-Rh/$Sn_{0.9}In_{0.1}P_2O_7$ three-way catalyst for propane + NO + O_2 reaction", **Xue Dong**, Kota Tsuneyama and Takashi Hibino*, *Applied Catalysis B*, 2011, 106, 503–509
3. "Compact bipolar plate-free direct methanol fuel cell stacks", **Xue Dong**, Motohiro Takahashi, Masahiro Nagao and Takashi Hibino*, *Chemical Communications*, 2011,47, 5292-5294

Conference Presentations

International Conference

1. "A Nano-sized Electrochemical Reactor for Propane+NO+O_2 Reaction", **Xue Dong**, Kota Tsuneyama and Takashi Hibino, *62nd Annual Meeting of the International Society of Electrochemistry, Japan.*
2. "Studies on novel self-organizing core-shell $VOMoO_4$/Mo-V-Te-O model catalysts with controllable bulk V^{4+} contents: exploring roles of bulk oxygen defects", Yihan Zhu, **Xue Dong**, Weimin Lu*, ***Poster***, *14th International Congress on Catalysis, Korea*

Domestic Conference

1. "Catalytic roles of Cr-doping in the $TeMo_5O_{16}$ catalyst", **Xue Dong**, Yihan Zhu, Weimin Lu, ***Oral Presentation***, *14th National Congress on Catalysis, China.*

2. "Crystal structure of self-organizing core-shell nano-$VOMoO_4$/MoVTeO catalyst" Yihan Zhu, **Xue Dong**, Weimin Lu*, ***Poster***, *14th National Congress on Catalysis, China.*

3. "*Ab initio* structure determination of self-organizing core-shell $VOMoO_4$/MoVTeO catalyst by powder diffractometry" ,Yihan Zhu, **Xue Dong**, Guanglie Lv, Weimin Lu*, ***Oral Presentation*** *(Cover Story), 4th National Congress of Chinese Crystallography Society, China.*

Acknowledgements

I would like to take this opportunity to thank all those who supported me technically or morally during my doctoral course.

I really thank Prof. Dr. Takashi Hibino, my guide and supervisor, who gave me a great chance to carry this interesting subject, and guide me to the art of experimenting. I acquired not only the knowledge of catalysis and electrochemistry, but also the ability to solve problems. I am deeply indebted to him for his earnest guidance, sincere encouragement and excellent research environments during the doctoral course at Nagoya University. He also kindly helps me a lot in my life from my application of the doctoral course to the graduation process.

I would like to thank Prof. Dr. Shizuaki MURATA, Prof. Dr. Shoichi IWAMATSU, and Prof. Dr. Anatoly ZINCHENKO for reviewing this thesis, and giving valuable comments.

I gratitude goes to Assistant Prof. Masahiro NAGAO, Dr. Yongcheng JIN and Dr. Yanbai SHEN for their kind advices on the study and their collaboration in Hibino Lab. Dr. SHEN shared his expertise and knowledge with me, and helped me in all the details of the experimental with kindness. I would also thank technical assistance member Kazuyo KOBAYASHI in Hibino Lab for her help in my research and life.

During the three years, I had the pleasure of meeting and working with so many great people. I would like to express my appreciation and thanks to graduate students in Hibino Lab. in Nagoya University: Dr. Byungik LEE, Mr. Kota TSUNEYAMA, Mr. Takahashi TAKEUCHI, Mr. Motohiro TAKAHASHI, Mr. Lu YANG, Mr.Masakazu

OKADA, Mr. Yousuke SATO, Mr. Keijiro KOJIMA, Mr Kenichi ITO, Mr Hiroto NAITO, Mr. Souhei NAKAI, and Mr. Ryou NOGIMURA. We have spent much time for the studies in Hibino Lab. and helped each other on some matters. My special thanks go to Mr. TSUNEYAMA, not only for his help in the experimental but also for his inspiriting attitude at work.

I would like to thank my friend in Japan. They supported me a lot in my life and cheered my up in the tough times. I also would like to thank my friend in China. Although we are far apart, my friend gave me a lot advice and support through the internet and telephone. I missed you so much.

Finally, and most importantly, it's my pleasure to express gratitude to my parents and other family members. They are my motive to keep move on and learn more. Without their continuous support, it would have been impossible for me to finish my research.

Xue DONG
Nagoya, Japan, 2013